

RESEARCH ARTICLE

10.1002/2017JG003932

Key Points:

- Using a data-model fusion approach, we constrained parameters and quantified uncertainties of CH₄ emission forecast
- Both warming and elevated air CO₂ concentrations have a stimulating effect on CH₄ emission
- The uncertainty in plant-mediated transportation and ebullition increased under warming

Correspondence to:

Y. Luo,
yiqi.luo@nau.edu

Citation:

Ma, S., Jiang, J., Huang, Y., Shi, Z., Wilson, R. M., Ricciuto, D., ... Luo, Y. (2017). Data-constrained projections of methane fluxes in a northern Minnesota peatland in response to elevated CO₂ and warming. *Journal of Geophysical Research: Biogeosciences*, 122, 2841–2861. <https://doi.org/10.1002/2017JG003932>

Received 18 MAY 2017

Accepted 12 OCT 2017

Accepted article online 20 OCT 2017

Published online 6 NOV 2017

Data-Constrained Projections of Methane Fluxes in a Northern Minnesota Peatland in Response to Elevated CO₂ and Warming

Shuang Ma¹ , Jiang Jiang^{2,3}, Yuanyuan Huang^{3,4}, Zheng Shi³ , Rachel M. Wilson⁵ , Daniel Ricciuto⁶ , Stephen D. Sebestyen⁷ , Paul J. Hanson⁶ , and Yiqi Luo^{1,8}

¹Center for Ecosystem Science and Society, Department of Biological Sciences, Northern Arizona University, Flagstaff, AZ, USA, ²Department of Soil and Water Conservation, Nanjing Forestry University, Nanjing, China, ³Department of Microbiology and Plant Biology, University of Oklahoma, Norman, OK, USA, ⁴Laboratoire des Sciences du Climat et de l'Environnement, Gif-sur-Yvette, France, ⁵Earth, Ocean and Atmospheric Sciences, Florida State University, Tallahassee, FL, USA, ⁶Environmental Sciences Division and Climate Change Science Institute, Oak Ridge National Laboratory, Oak Ridge, TN, USA, ⁷U.S. Forest Service, Northern Research Station, Center for Research on Ecosystem Change, Grand Rapids, MN, USA, ⁸Department of Earth System Science, Tsinghua University, Beijing, China

Abstract Large uncertainties exist in predicting responses of wetland methane (CH₄) fluxes to future climate change. However, sources of the uncertainty have not been clearly identified despite the fact that methane production and emission processes have been extensively explored. In this study, we took advantage of manual CH₄ flux measurements under ambient environment from 2011 to 2014 at the Spruce and Peatland Responses Under Changing Environments (SPRUCE) experimental site and developed a data-informed process-based methane module. The module was incorporated into the Terrestrial Ecosystem (TECO) model before its parameters were constrained with multiple years of methane flux data for forecasting CH₄ emission under five warming and two elevated CO₂ treatments at SPRUCE. We found that 9°C warming treatments significantly increased methane emission by approximately 400%, and elevated CO₂ treatments stimulated methane emission by 10.4%–23.6% in comparison with ambient conditions. The relative contribution of plant-mediated transport to methane emission decreased from 96% at the control to 92% at the 9°C warming, largely to compensate for an increase in ebullition. The uncertainty in plant-mediated transportation and ebullition increased with warming and contributed to the overall changes of emissions uncertainties. At the same time, our modeling results indicated a significant increase in the emitted CH₄:CO₂ ratio. This result, together with the larger warming potential of CH₄, will lead to a strong positive feedback from terrestrial ecosystems to climate warming. The model-data fusion approach used in this study enabled parameter estimation and uncertainty quantification for forecasting methane fluxes.

Plain Language Summary Methane (CH₄) has 45 times the sustained-flux global warming potential of CO₂ over a 100-year scale, and it is directly responsible for approximately 20% of global warming since pre-industrial time. Wetlands are the single largest natural source of CH₄ emission and there is major concern about potential feedbacks between global climate change and CH₄ emissions from wetlands, as warming and atmospheric CO₂ are known to affect CH₄ emissions. However, extensive observed CH₄ flux data have not been well used to constrain model predictions of CH₄ emission in the future climate. Using a data-model fusion approach, we constrained parameters and quantified uncertainties of CH₄ emission forecast. We found both warming and elevated air CO₂ concentrations have a stimulating effect on CH₄ emission. The uncertainty in plant-mediated transportation and ebullition increased under warming.

1. Introduction

Methane (CH₄) is the simplest hydrocarbon produced by anaerobic microbes in the terminal step of organic matter remineralization. CH₄ has 45 times the sustained-flux global warming potential of CO₂ over a 100 year scale (Neubauer & Megonigal, 2015), and it is directly responsible for approximately 20% of global warming since preindustrial periods (Forster et al., 2007). Wetlands are the single largest natural source of emitted CH₄ (Bridgman et al., 2013), and there is major concern about potential feedbacks between global climate change and CH₄ emissions from wetlands, as warming and atmospheric CO₂ are known to affect CH₄ emissions

(Bridgman et al., 2006; Zhuang et al., 2004). However, extensive observed CH₄ flux data have not been well used to constrain model predictions of CH₄ emission in the future.

Process-based biogeochemistry models have been used to quantify global wetland CH₄ emissions with different complexities in model structures (Cao, Dent, & Heal, 1995; Riley et al., 2011; Walter & Heimann, 2000; Wania, Ross, & Prentice, 2010; Zhang et al., 2002; Zhu et al., 2014; Zhuang et al., 2004). However, large uncertainties exist in predicting responses of methane emissions to future climate change (Bridgman et al., 2013; Frolking, Roulet, & Fuglestedt, 2006). In methane models, the uncertainties in model predictions stem from the following:

Model structure. Process-based models with more details and controls are being developed at the site level and will be added into global models, but a bottleneck is the lack of spatially explicit physical, chemical, and biological data (Bridgman et al., 2013).

Parameter values. Some conceptual parameters used in methane models are not directly measurable, and there is a limited variety of observational data that do not comprehensively address various CH₄ emission pathways that are needed to constrain parameter values using data assimilation.

Forcing data (Luo et al., 2015). Water table level and soil temperature are the two dominant controls on methane flux simulation because (a) the water table position determines the extent of the catotelm zone where methane is largely produced (acrotelms may be anoxic, and methane may be produced in acrotelm) and the acrotelm where most methane is oxidized (methane can also be oxidized by methanotrophs in catotelm using Fe³⁺, NO₃⁻, SO₄²⁻, etc., as electron acceptors) (Bartlett et al., 1990; Dise et al., 1993; Bubier et al., 1995; Walter & Heimann, 2000) and (b) soil temperature affects the rates of microbiological processes such as fermentation, methanogenesis, and methanotrophy (Dise et al., 1993; Frolking & Crill, 1994; Kettunen et al., 1999; Walter & Heimann, 2000).

Biogeochemical models and experimental results are generally consistent in showing that climate warming stimulates CH₄ emissions. Modeling results under +1 and +2°C warming scenarios found increases in CH₄ emission in northern wetlands by 17% and 11% but decreases under higher elevated temperature due to the effect of soil moisture depletion (Cao, Gregson, & Marshall, 1998). Short-term warming and coupled water table level × warming in situ or mesocosm manipulations have been used at the site level to explore the responses of northern peatland CH₄ emission to climate warming from +0.6 to +2.0°C. These studies found that warming increased CH₄ fluxes by 15%–550% or had no effect based on the condition of water table variation and vegetation change (Granberg et al., 2001; Turetsky et al., 2008; Updegraff et al., 2001; Verville et al., 1998). However, these studies only warmed the soil surface, which may have precluded deep soil responses to warming especially in northern wetlands where a significant fraction of C is stored in deep peat layers. Nevertheless, methane fluxes measured under warming or elevated CO₂ (eCO₂) have never been incorporated into models via data-model fusion or used to constrain models in projecting methane emission under climate change.

Net methane emission includes contributions from plant-mediated transport, diffusion, and ebullition (i.e., bubble release). Over 90% of the methane emission in a *Carex*-dominated fen near Schefferville, Quebec, Canada, was mediated by plants (Whiting & Chanton, 1992). Emergent plants in a peatland in southern Michigan, USA, accounted for 64%–90% of the net CH₄ efflux in plant enclosure experiments (Shannon et al., 1996). Plant-mediated fluxes averaged 69.8 ± 11.8 mg CH₄ m⁻² d⁻¹ and accounted for ~50% of total fluxes at the Alaska Peatland Experiment site (Shea, Turetsky, & Waddington, 2010). In the same study, diffusion contributed to less than 9% of total CH₄ flux (up to 7.6 mg CH₄ m⁻² d⁻¹) and ebullition accounted for ~41% of total CH₄ flux. However, the quantity and temporal-spatial scales of experimental studies are limited, so the responses of the relative contributions of the three processes to climate warming have not been unraveled either using experiments or modeling approaches.

In process-based methane models, the individual pathway of CH₄ emission is related to CH₄ pool size (CH₄ concentration), which is primarily determined by CH₄ production. Once the parameters in CH₄ production, plant-mediated transportation, ebullition, and diffusion are constrained by observed data and the prior range of parameter values with a data-model fusion technique (Keenan et al., 2011, 2012; Richardson et al., 2010; Smith et al., 2013; Wang, Trudinger, & Enting, 2009), the simulation of differential contributions from the three pathways under warming and eCO₂ may be improved. The Spruce and Peatland Responses Under Changing Environments (SPRUCE) experimental site is unique in coupling deep peat heating (to a depth of 2 m) and

aboveground warming at +0°C, +2.25°C, +4.5°C, +6.75°C, and +9°C above ambient temperature along with eCO₂ treatment (Hanson et al., 2016). Although not enough data are yet available for validating methane emission under warming treatments, the extensive data sets released or coming out from SPRUCE will enable parameter estimation, uncertainty quantification, and contribution from each pathway to better forecast methane fluxes under warming and eCO₂.

In this study, we focus on developing a data-informed process-based model using the methane chamber measurement data from a northern peatland in northern Minnesota where the SPRUCE project is occurring. We also looked at differential responses of CH₄ production, oxidation, diffusion, ebullition, and plant-mediated transportation to warming and eCO₂. We hypothesized that both warming and eCO₂ would increase methane emission in this ombrotrophic bog, with differential responses of each process due to the differential temperature dependencies of methanogenesis and respiration.

2. Methods

2.1. Site Description and Treatments

We took Spruce and Peatland Responses Under Climatic and Environmental Change experiment (SPRUCE) as our case study site. The SPRUCE project is conducted to study the responses of northern peatland to climate warming (+0, +2.25, +4.5, +6.75, and +9°C) and elevated atmospheric CO₂ concentration (+0 and +500 ppm) (Hanson et al., 2016). The SPRUCE experiment is located in the 8 ha S1 Bog that has been at the Marcell Experimental Forest (MEF, N47°30.476', W93°27.162', 418 m above mean sea level), a site in northern Minnesota, USA, with a long-term research program that is administered by the U.S. Department of Agriculture (USDA) Forest Service. Temperature and precipitation have been measured since 1961 at the MEF South Meteorological station, which is about 1 km from the SPRUCE experiment. The mean annual temperature from 1961 to 2009 was 3.4°C, and the mean annual precipitation was 780 mm (Sebestyen et al., 2011). Mean annual air temperatures have increased approximately 0.4°C per decade over the last 50 years (Sebestyen et al., 2011). Vegetation within the S1 Bog is dominated by trees species *Picea mariana* and *Larix laricina*, a variety of ericaceous shrubs, and *Sphagnum* sp. moss. The bog also has graminoids *Carex trisperma* and *Eriophorum spissum*, as well as forbs *Sarracenia purpurea* and *Smilacina trifolia*. Mean peat depth in this bog is around 2–3 m (Parsekian et al., 2012).

The water table typically fluctuates within the top 30 cm of peat at five long-studied bogs on the MEF (Sebestyen, Verry, & Brooks, 2011). Within SPRUCE, water table levels have been measured half hourly (except during freezing temperatures) at the meteorological station EM1 on the southwest side of the experiment site since January 2011. The sensor was placed in a hollow (microtopographic lows that are interspersed among hummocks of bogs (Verry, 1984)). A TruTrack WT-VO water level sensor was used to measure water table levels that were logged with a Campbell Scientific CR1000 data logger. In this study, water table height is expressed as zero at the hollow surface during late spring or early summer (Sebestyen & Griffiths, 2016). Community level CH₄ emissions were measured once each month during snow-free months beginning during 2011 using a portable open-path analyzer in each plot at “large collars” (area of 1.13 m²) that have been previously described (Hanson et al., 2016, 2017). Mean annual air temperature at 2 m height ranged 1.91–5.10°C, mean annual soil temperature at 30 cm depth ranged 5.83–7.06°C, and annual precipitation ranged 651–717 mm during the year 2011–2016. In total, 45 daily CH₄ chamber measurement data points were integrated from ambient plots from 2011 to 2016. We took the mean value if there are more than one plot that have data on the same date; variations in different ambient plots were not simulated due to our purpose to represent the site level CH₄ emission.

2.2. Model Description and Key Processes

2.2.1. Overview of TECO

The process-based biogeochemistry model, TECO (Terrestrial ECOSystem model), simulates carbon, nitrogen, and hydrology cycles in terrestrial ecosystems (Weng & Luo, 2008). The model has four major components: canopy photosynthesis, soil water dynamics, plant growth (allocation and phenology), and soil carbon and nitrogen transfers. A detailed description of TECO is available in Weng and Luo (2008) and Shi et al. (2015). The canopy submodule was mainly derived from Wang and Leuning's (1998) two-leaf model, which simulated processes of canopy photosynthesis, conductance, energy balance, and transpiration. The soil water dynamics submodule has 10 soil layers and simulates soil moisture dynamics based on precipitation, evapotranspiration, and runoff. Evaporation is regulated by the first soil layer water

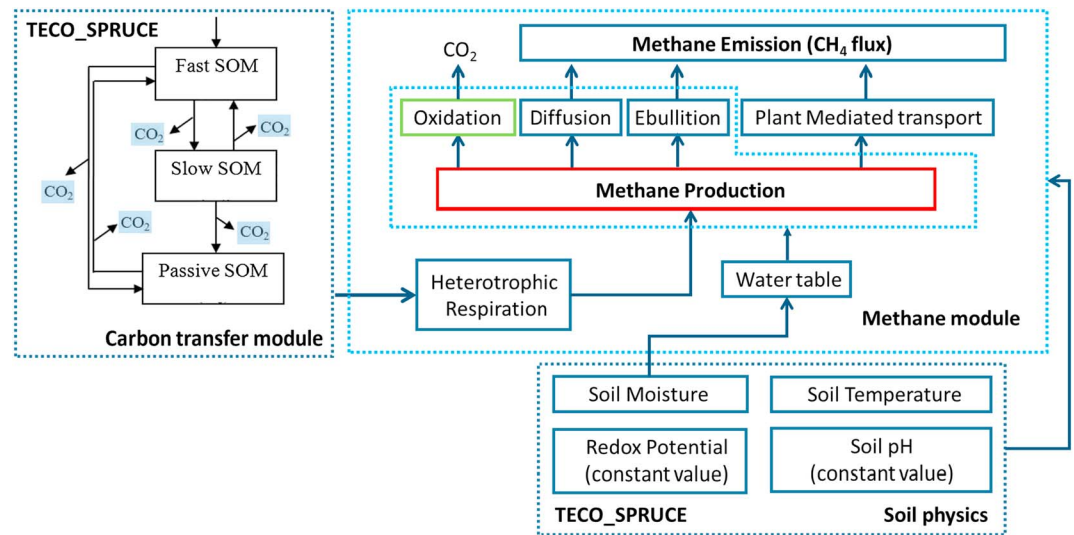


Figure 1. Conceptual structure and integration of water table and CH₄ emission modules into TECO_SPRUCE.

content and the evaporative demand of the atmosphere. Transpiration is determined by stomatal conductance and the soil water content of layers where roots are present. When precipitation exceeds water recharge to soil water holding capacity, runoff occurs. The C transfer submodule simulates movement of C from plants to three soil C pools through litterfall and the decomposition of litter and soil organic C. Carbon fluxes from litter and soil carbon pools are based on residence time of each C pool and the C pool sizes (Luo & Reynolds, 1999).

The TECO model has been adapted to the SPRUCE site to study the carbon dynamic (by Jiang Jiang) and soil thermal dynamic (by Huang et al., 2017). The documentation of the constrained model for the SPRUCE site is available from the GitHub repository (<https://github.com/ou-ecolab>), and the model performance can be found at the Ecological Platform for Assimilation of Data into models (EcoPAD) (http://ecolab.cybercommons.org/ecopad_portal/). Since water table is an important variable determining aerobic and anaerobic below-ground environments and further influence CH₄ production, oxidation, and diffusion, we improved the model by incorporating hourly time step water table dynamics and methane production, oxidation, diffusion, ebullition, and plant-aided transportation processes into the model. We followed the original TECO_SPRUCE structure and divided the soil into 10 layers, with the first five layers that were 10 cm thick and the other five layers that were 20 cm thick (most peatland roots are distributed in the top 60 cm peat layer). The conceptual structure of water table and methane flux models and the incorporation into TECO_SPRUCE are shown in Figure 1 and further described below.

2.2.2. Water Table Module

New algorithms were developed and integrated into the hydrological part of TECO to estimate the water table level and the influence of the water table on soil moisture in the unsaturated zone. Generally, the water table module followed Granberg et al.'s (1999) method and this approach has been widely applied in global methane models (Zhuang et al., 2004; Wania, Ross, & Prentice, 2009a; Zhu et al., 2014). Based on our observation data, these bog soils are always saturated below 30 cm (Tfaily et al., 2014), except during some extreme droughts (Sebestyen et al., 2011). Therefore, we set 30 cm as the maximum water table depth (z_b). The system was considered as a simple bucket model. The changes in water content of the top 30 cm soil profile can be calculated by a water balance model characterized by water input and output at hourly time step. The level of the water table is determined by soil moisture change. We used a constructed function for water-holding capacity to simulate the dynamics of the water table level. In the unsaturated zone, we use a quadratic function and the soil volumetric water content (θ_{us}) increases from the vegetation surface volumetric water content (θ_s) to the position of the water table (z_{wt}) as follows:

$$\theta_{us}(z) = \min \left[\varphi, \theta_s + (\varphi - \theta_s) \left(\frac{z}{z_{wt}} \right)^2 \right], \quad (1)$$

where φ has a constant value of 0.95, z is the depth in soil (mm), and θ_s is adapted from Hayward and Clymo (1982) and represented as

$$\theta_s = \max [\theta_{s \min}, \varphi - (a_z z_{wt})], \quad (2)$$

where $\theta_{s \min}$ is the minimum volumetric water content still held by capitulum of *Sphagnum* at the soil surface and set to 0.25, a_z is the linearly decreasing gradient given by

$$a_z = \frac{\varphi - \theta_{s \min}}{z_{\theta_{s \min}}}, \quad (3)$$

where $z_{\theta_{s \min}}$ is the maximum suction interval given the value 100 mm. Thus, the total volume of water in soil profile above z_b would be

$$V_{\text{tot}} = \varphi(z_b - z_{wt}) + \int_0^{z_{wt}} \theta_{us}(z) dz, \quad (4)$$

where the first part of the equation represents the water content in the saturated zone above z_b , and the second part of the equation refers to the water content in the unsaturated zone. If the whole profile is saturated, the height of standing water is represented by the difference of V_{tot} and $z_b \varphi$. The final equation for water table depth is

$$z_{wt} = \begin{cases} \sqrt{\frac{3(\varphi z_b - V_{\text{tot}})}{2a_z}} & \text{if } z_{wt} > 0 \text{ and } z_{wt} \leq z_{\theta_{s \min}} \\ \frac{3(\varphi z_b - V_{\text{tot}})}{2(\varphi - \theta_{s \min})} & \text{if } z_{wt} > z_{\theta_{s \min}} \text{ and } z_{wt} < z_b, \\ -(V_{\text{tot}} - z_b \varphi) & \text{if } z_{wt} < 0 \end{cases} \quad (5)$$

where a positive value of z_{wt} indicates that the water table is below the hollow surface and a negative value of z_{wt} indicates that the water table is above the hollow surface.

2.2.3. Methane Module

TECO_SPRUCE_ME explicitly considers the transient and vertical dynamics of CH_4 production (P_{ro} , methanogenesis), CH_4 oxidation (O_{xi} , methanotrophy), and CH_4 transport from the soil to the atmosphere which includes ebullition (E_{bu}), diffusion (D_{ifu}), and plant-mediated transport (A_{ere}) in the soil profiles. The structure and processes were adapted from a number of previous studies and models (Riley et al., 2011; Walter & Heimann, 2000; Wania et al., 2010; Zhuang et al., 2004). We assume that soils can be separated into an unsaturated zone above the water table and a saturated zone below the water table. Methane oxidation occurs in the unsaturated zone and rhizosphere (as explained in section 2.2.3.4), and methane production occurs in the saturated zone (Cao, Marshall, & Gregson, 1996; Walter & Heimann, 2000; Zhu et al., 2014; Zhuang et al., 2004). To simulate methane dynamics within the soil, we divided the soil column into 10 layers, with the first five layers that were 10 cm thick and the other five layers that were 20 cm thick. Within each soil layer, CH_4 concentration dynamics were calculated by a transient reaction equation:

$$\frac{\partial([\text{CH}_4])}{\partial t} = P_{\text{ro}}(z, t) - O_{\text{xi}}(z, t) - E_{\text{bu}}(z, t) - A_{\text{ere}}(z, t) - \frac{\partial D_{\text{ifu}}(z, t)}{\partial z}, \quad (6)$$

where (CH_4) is soil CH_4 concentration (g C m^{-3}), z is the depth in soil (mm), t is time step (h), $P_{\text{ro}}(z, t)$ is the CH_4 production rate, $O_{\text{xi}}(z, t)$ is the CH_4 oxidation rate, $E_{\text{bu}}(z, t)$ is the ebullitive CH_4 emission rate, and $A_{\text{ere}}(z, t)$ is the plant-mediated transportation rate. The term $\frac{\partial D_{\text{ifu}}(z, t)}{\partial z}$ is the flux divergence resulting from the diffusion of methane into/out of soil layer z from the lower/upper soil layer or the atmosphere (for the first layer). A negative value indicates a reverse transfer direction determined by the difference of CH_4 concentration between adjacent layers. The total emission of CH_4 from soil to atmosphere ($F_{\text{CH}_4}(t)$) is represented as

$$F_{\text{CH}_4}(t) = E_{\text{bu}}(t) + A_{\text{ere}}(t) + D_0(t), \quad (7)$$

where within each time step, $E_{\text{bu}}(t)$ is the sum of all the ebullitive CH_4 emissions in soil layers, $A_{\text{ere}}(t)$ is the sum of all the plant-aided CH_4 emissions in soil layers, and $D_0(t)$ is the diffused flux from the first soil layer into the atmosphere (a negative value indicates diffused flux from the atmosphere into the soil).

2.2.3.1. Methane Production

Methanogenesis is the terminal step of soil organic carbon decomposition under anaerobic conditions (Conrad, 1999). This process is determined by carbon substrate supply and soil environmental conditions such as water table via O_2 availability and soil temperature (Walter & Heimann, 2000). In TECO_SPRUCE_ME, CH_4 production occurs only in the saturated zone of the soil profile. Similar to CLM4Me (Riley et al., 2011), LPJ-WHyMe (Spahni et al., 2011; Wania et al., 2010), and TRIPLEX-GHG (Zhu et al., 2014) models, we assume that there are no time delays between fermentation and methanogenesis so that CH_4 production within the catotelm is directly related to heterotrophic respiration from soil and litter (R_h , $g\ C\ m^{-2}h^{-1}$):

$$P_{ro}(z, t) = R_h(z, t)r_{me}f_{stp}(z, t)f_{pH}f_{red}, \quad (8)$$

where $R_h(z, t)$ is redistributed in different soil layers by assuming that 50% is associated with roots and the rest is evenly distributed among the top 0.3 m of soil (Riley et al., 2011). The distribution of root biomass was estimated from minirhizotrons and root in-growth cores over the summer of 2013 (Iversen et al., 2017). The fractions of root biomass in each soil layer ($f_{root}(z)$) were estimated as 0.1, 0.25, 0.25, 0.2, 0.1, 0.05, 0.025, 0.015, 0.005, and 0.005 from the upper boundary (the soil surface or water surface if the water table is above the soil surface) to a lower boundary. The parameter r_{me} is the potential ratio of anaerobically mineralized C released as CH_4 , which is an ecosystem-specific conversion scaler. The soil environmental scalars, f_{stp} , f_{pH} , and f_{red} are for soil temperature, pH and redox potential. The factor f_{stp} is a multiplier enhancing CH_4 production with increasing soil temperature. It uses a Q_{10} function with a Q_{10} coefficient for production (Q_{10pro}), a highest temperature (T_{max}) and optimum temperature (T_{opt}) for CH_4 production. We used Q_{10pro} which refers to a parameter that describes the temperature sensitivity of the reaction from CO_2 to CH_4 . Q_{10Rh} describes temperature sensitivity of the reaction from soil organic carbon to CO_2 , which has already been adapted and constrained (by Jiang Jiang). Previous studies have shown that in winter when soil temperature is below $0^\circ C$, the methanogenesis rate is significantly lower than that of the rates observed during growing seasons (Shannon & White, 1994; Whalen & Reeburgh, 1992). Therefore, CH_4 production in the model only occurs when soil temperature is above $0^\circ C$ and below an extremely high temperature of $45^\circ C$ as shown below:

$$f_{stp}(t) = \begin{cases} 0 & \text{if } T_{soil} < 0 \\ \frac{Q_{10pro}}{10} \frac{T_{soil}(t) - T_{optpro}}{10} & \text{if } 0 \leq T_{soil} \leq T_{max} \\ 0 & \text{if } T_{soil} > T_{max} \end{cases}, \quad (9)$$

where $T_{soil}(t)$ is the hourly soil temperature and T_{optpro} is the optimum temperature for CH_4 production, which varies across ecosystems. In this study we chose a value of $20^\circ C$ since this was the maximum temperature for which methane production was examined in incubations of peat from this site (Wilson et al., 2016).

The factors f_{pH} and f_{red} are nominally set to a constant value of 1.0 due to the model sensitivity (Meng et al., 2012; Riley et al., 2011) and uncertainty in characterizing these two parameters (Le Mer & Roger, 2001; Wania et al., 2010; Whalen, 2005). In the CLM4Me model, the effect of pH and redox potential on net fluxes were tested in the sensitivity analysis and resulted in less than a 20% change in net CH_4 emission at high latitudes (Riley et al., 2011). Redox potential does not have substantial impacts on methane emissions at seven wetland sites including one adjacent to the Marcell Experimental Forest in north central Minnesota (Meng et al., 2012; Shurpali & Verma, 1998). Wania et al. (2010) argued that the pH and redox factors are so poorly characterized that they should be excluded. Many of the current process-based methane models use a single value for the pH scaler calculated from the soil property that does not change with time and depth. In many process-based methane models a step function is used for calculating the redox potential scaler (Fiedler & Sommer, 2000; Segers & Kengen, 1998; Zhang et al., 2002), which is decided by root distribution, fraction of water-filled pore space, the water table position, and several other constant parameters with a single value across different ecosystems such as change rate of soil redox potential under saturated conditions, cross-sectional area of a typical fine root, and fine root length density. In our model, the potential ratio of anaerobically mineralized C released as CH_4 can reflect some of the information on the effects of pH and redox potential to methane production. We kept f_{pH} and f_{red} in equation (8) because as more information become available, we might be able to improve their calculation in our later versions.

2.2.3.2. Methane Oxidation

Methane is oxidized by methanotrophs in both the acrotelm (O_2 as electron acceptor) and the catotelm (Fe^{3+} , NO_3^- , SO_4^{2-} , etc., as electron accepters). Like in other methane models (Cao et al., 1996; Zhuang et al., 2004), we only consider CH_4 oxidation in the acrotelm and during the process of plant-mediated transportation (as explained in section 2.2.3.4). Given that CH_4 oxidation is largely controlled by CH_4 concentration, it is assumed to follow the Michaelis-Menten kinetics (Bender & Conrad, 1992) represented by

$$O_{xi}(z, t) = O_{max} f_{CH_4}(z, t) f_{sto}(z, t), \quad (10)$$

where O_{max} is the ecosystem-specific maximum oxidation rate ($\mu\text{mol L}^{-1} \text{h}^{-1}$) for CH_4 , f_{CH_4} is the CH_4 concentration coefficient equal to $\frac{[CH_4](z, t)}{K_{CH_4} + [CH_4](z, t)}$, where $[CH_4]$ denotes the soil methane concentration (g C m^{-3}) at time t and depth z , and K_{CH_4} is Michaelis constant. $f_{sto}(z, t)$ is an environmental scaler associated with a Q_{10} function, with Q_{10oxi} and ecosystem-specific optimum temperature for oxidation (T_{optoxi}).

2.2.3.3. Aqueous and Gaseous Diffusion

In process-based models, CH_4 emission from the soil to the atmosphere is represented by three pathways: diffusion ($D_{if}(z, t)$), plant-mediated transport ($A_{ere}(z, t)$), and ebullition ($E_{bu}(z, t)$).

The CH_4 diffusion across soil layers follows Fick's first law,

$$D_{ifu}(z, t) = D_{CH_4}(z, t) \frac{\partial [CH_4](z, t)}{\partial z}, \quad (11)$$

where $D_{ifu}(z, t)$ is the diffusive flux at depth z (mm) and time t (hour) and $[CH_4](z, t)$ is the corresponding methane concentration (g C m^{-3}). The diffusion coefficient ($D_{CH_4}(z, t)$) varies with soil layers, and the calculation is adapted and modified from Walter and Heimann (2000):

$$\frac{D_{coe}(z, t) = (f_{air}(z, t))^{10/3}}{\varphi^2 \times D_{CH_4a}}, \quad (12)$$

$$D_{CH_4}(z, t) = \begin{cases} D_{CH_4w}, & f_{air}(z, t) \leq 0.05, \\ D_{coe}(z, t), & f_{air}(z, t) > 0.05. \end{cases} \quad (13)$$

where $D_{coe}(z, t)$ is the CH_4 diffusivity in soil, D_{CH_4a} and D_{CH_4w} are the diffusion coefficient of methane in bulk air ($0.2 \text{ cm}^2 \text{ s}^{-1}$) and in water ($0.2 \cdot 10^{-4} \text{ cm}^2 \text{ s}^{-1}$) (Walter & Heimann, 2000), φ is soil porosity, f_{water} is the fraction of water-filled pore space in soil calculated from soil water content, and f_{air} is the fraction of air-filled pore space in soil calculated by $\varphi - f_{water}$. Only the net emission or uptake from first layer ($D_0(t)$) directly contributes to the final CH_4 flux exchange between soil and the atmosphere. For boundary conditions, the methane flux at the bottom boundary was set to zero. The atmospheric CH_4 concentration at the soil surface (or water surface if the water table is at or above the soil surface) is set to $0.076 \mu\text{M}$. At the water-air interface the methane concentrations in both phases are assumed to be in equilibrium. For layers where air fraction ($f_{air}(z, t)$) < 0.05 , the diffusivities for water were used. When $f_{air}(z, t) > 0.05$, the diffusivities in soil were used.

2.2.3.4. Plant-Mediated Transportation

Vascular plants enhance CH_4 emissions by transporting CH_4 from the point of methanogenesis in the rhizosphere directly to the atmosphere (Joabsson, Christensen, & Wallén, 1999). When gas is transported through intercellular spaces (molecular diffusion) or aerenchyma tissues, methane emissions are larger than through diffusion alone because the diffusive CH_4 flux may bypass the soil profiles where it might otherwise be consumed above water table level by oxygen (O_2) or below the interface by Fe^{3+} , NO_3^- , SO_4^{2-} , etc. (Chanton & Dacey, 1991). Conversely, plants could reduce CH_4 emissions by releasing O_2 to the rhizosphere thereby enhancing CH_4 oxidation. In TECO_SPRUCE_ME, plant-mediated transport is adapted from Walter's model (Walter & Heimann, 2000). We described two processes: CH_4 transported through plants and directly into the atmosphere (the "chimney effect") and enhanced CH_4 oxidation during upward transport in tissues. Briefly, it is modeled as a function of the vegetation condition (T_{veg}), the fraction of root biomass in each soil layer ($f_{root}(z)$), the growing state of plants ($f_{growth}(t)$), the fraction of CH_4 consumed by oxidation in rhizosphere (P_{ox}), and the distribution of soil CH_4 concentrations in the soil:

$$A_{ere}(t) = k_{pla} T_{veg} f_{root}(z) f_{growth}(t) [CH_4] (1 - P_{ox}), \quad (14)$$

where k_{pla} is a rate constant with the unit 0.01 h^{-1} . The parameter T_{veg} is a factor of transport ability at the plant community level, which is set by species composition and plant density. The fraction of CH_4 consumed by oxidation in rhizosphere, P_{ox} , is set to 50%, although there is high variability of observed values (Gerard & Chanton, 1993; Schipper & Reddy, 1996). The multiplier $f_{\text{growth}}(t)$ describes the effects of the growing stage of vegetation on plant-mediated methane transport (Walter & Heimann, 2000; Zhuang et al., 2004); it is determined by leaf area index (LAI) and soil temperatures (T_{soil})

$$f_{\text{growth}}(t) = \begin{cases} \text{LAI}_{\text{min}} & \text{if } T_{\text{soil}} < T_{\text{gr}} \\ \text{LAI}_{\text{min}} + \text{LAI}_{\text{max}} \left(1 - \left(\frac{T_{\text{mat}} - T_{\text{soil}}}{T_{\text{mat}} - T_{\text{gr}}} \right)^2 \right) & \text{if } T_{\text{gr}} \leq T_{\text{soil}} \leq T_{\text{mat}}, \\ \text{LAI}_{\text{max}} & \text{if } T_{\text{mat}} > T_{\text{soil}} \end{cases} \quad (15)$$

where LAI_{min} is the minimum LAI associated with the beginning of plant growth, while LAI_{max} is the maximum LAI associated with plant at maturity. We used T_{gr} as the temperature at which plants starts to grow, and T_{mat} is the temperature at which plants reach maturity. Similar to Walter and Heimann (2000) and Zhuang et al. (2004), LAI_{min} and LAI_{max} were chosen to be 0 and 4, respectively. T_{gr} is equal to 7°C where the annual mean soil temperature is above 5°C ; otherwise, T_{gr} is equal to 2°C . The annual mean soil temperature at our study site is $5.83\text{--}7.06^\circ\text{C}$, so the value 7°C was used. T_{mat} is assumed to equal $T_{\text{gr}} + 10^\circ\text{C}$.

A range of 0–15 for T_{veg} was used in a process-based model at five wetland sites (Walter & Heimann, 2000). In Zhuang et al. (2004), the value of T_{veg} was given as 0.5 for tundra ecosystems and 0.0 for boreal forests, as they considered trees to not contribute to plant-mediated transport; shrubs to mediate some gas transportation; and grasses, ferns, and sedges to be good mediators of gas transport. The assignments of this parameter are empirical and would be improper for trees and shrubs that mediate CH_4 transportation. In our study we give a 0–15 range for T_{veg} from those studies and try to constrain the value by using data assimilation as illustrated below.

2.2.3.5. Ebullition

We assumed that bubbles form when the CH_4 concentration exceeded a certain threshold ($[\text{CH}_4]_{\text{thre}} = 750 \mu\text{mol L}^{-1}$) (Walter & Heimann, 2000) and that bubbles were directly emitted into the atmosphere when the water table was above the soil surface. Otherwise, the bubbles are added to the soil layer just above the water table and then continue to diffuse through the soil layers if z is below the water level:

$$E_{\text{bu}}(z, t) = \begin{cases} K_{\text{ebu}}([\text{CH}_4](z, t) - [\text{CH}_4]_{\text{thre}}) & \text{if } [\text{CH}_4] > [\text{CH}_4]_{\text{thre}} \\ 0.0 & \text{if } [\text{CH}_4] \leq [\text{CH}_4]_{\text{thre}} \end{cases}, \quad (16)$$

where K_{ebu} is a rate constant of 1.0 h^{-1} (Walter & Heimann, 2000). No bubbles are formed if z is above the water level.

2.3. Sensitivity Test for Data Assimilation

The efficiency of data assimilation is affected by the number of observational data sets and the amount of data in each set. In this study, methane emission data are the only available observational data sets for data assimilation. Therefore, we chose only the most sensitive parameters for data assimilation because the observational variable is usually sensitive to the changes in parameter values when a parameter can be constrained by that variable in data assimilation (Roulier & Jarvis, 2003). We chose nine key parameters used in TECO_SPRUCE_ME (Table 1) for the initial sensitivity test, and most of the remaining parameters are physical constants. The sensitivity of parameters is determined by sensitivity index (I) defined as

$$I = \frac{(y_2 - y_1)/y_0}{2\Delta x/x_0}, \quad (17)$$

where y_0 is the model output (methane emission) with an initial value of the independent variable x_0 (parameters in Table 1). The independent variable value varied by $\pm\Delta x$ with corresponding dependent variable values y_2 and y_1 . Δx was set at 0.25 times of initial values. The sensitivity index (I) was used by Lenhart et al. (2002) and Zhu et al. (2014) to quantify sensitivity, which was ranked into four levels; the grading of the index could be found in Lenhart et al. (2002).

Table 1
Major Parameters in CH₄ Production, Oxidation, Diffusion, Ebullition, and Plant-Mediated Transportation

Process	Parameters	Values	Range	Unit	Description	References
CH ₄ production	r_{me}	0.65	[0.0, 0.7]	-	Potential ratio of anaerobically mineralized C released as CH ₄	Zhuang et al. (2004), Segers (1998), and Zhu et al. (2014)
	Q_{10_pro}	7.2	[0.0, 10]	-	Q ₁₀ for CH ₄ production	Walter and Heimann (2000)
CH ₄ oxidation	Topt_pro	20.0	-	°C	Optimum temperature for CH ₄ production	Wilson et al. (2016)
	K_{CH4}	5.0	-	μmol L ⁻¹	Michaelis-Menten coefficients	Walter and Heimann (2000) and Zhang et al. (2002), Zhuang et al. (2004)
	O_{max}	15.0	[3.0, 45.0]	μmol L ⁻¹ h ⁻¹	Maximum oxidation rate	Walter and Heimann (2000) and Meng et al. (2012)
	Q_{10_oxi}	2.0	-	-	Q ₁₀ for CH ₄ oxidation	Walter and Heimann (2000) and Meng et al. (2012)
CH ₄ diffusion	Topt_oxi	10.0	-	°C	Optimum temperature for CH ₄ production	Zhuang et al. (2004)
	f_{tort}	0.66	-	-	Tortuosity coefficient	Walter and Heimann (2000)
	D_{air}	0.2	-	cm ² s ⁻¹	Molecular diffusion Coefficient of CH ₄ in air	Walter and Heimann (2000)
	D_{water}	0.00002	-	cm ² s ⁻¹	Molecular diffusion coefficient of CH ₄ in water	Walter and Heimann (2000)
CH ₄ Ebullition	[CH₄]thre	750	-	μmol L ⁻¹	CH ₄ concentration threshold above which ebullition occurs	Walter and Heimann (2000) and Zhu et al. (2014)
Plant-mediated transportation	T_{veg}	0.7	[0.01, 15.0]	-	Factor of transport ability at plant community level	Walter and Heimann (2000) and Zhuang et al. (2004)

Note. Parameters in bold indicate the ones used for initial sensitivity test. Parameters with a range indicate the model is sensitive to their values and are used for data assimilation.

2.4. Data Assimilation

Using the Bayesian probabilistic inversion technique, we estimated the posterior distribution of model parameters based on prior knowledge of parameter ranges (Table 1) and field chamber measurements of CH₄ emissions. Since the whole-ecosystem warming (air heating and deep peat heating) treatments were recently initiated on 12 August 2015 (Hanson et al., 2017), and the number of whole-ecosystem warming treatment data points were not enough for data assimilation, we only compiled chamber measurement data in ambient plots from 2011 to 2014 for data assimilation and 2015 to 2016 for validation. Both the observed data and simulated results were rescaled to a daily emission unit for comparison. In order to project future methane flux uncertainty only related to parameter values, we conducted 100 forecasting runs by randomly choosing parameter sets from their posterior distributions, and we randomly picked one set of stochastically generated environmental variables and used the same set for all the forecasting runs.

Bayes' theorem provides an equation in which the posterior probability density function $p(\theta|Z)$ of model parameters for given observations Z is based on prior knowledge of parameter distribution $p(\theta)$ and the likelihood function $p(Z|\theta)$:

$$p(\theta|Z) \propto p(Z|\theta)p(\theta), \quad (18)$$

Here we assume that the prior knowledge of parameter distribution $p(\theta)$ is uniformly distributed. Due to the equifinality and unidentifiable parameters when using only one observation data stream to constrain multiple parameters (Luo et al., 2009), we only chose four parameters with high sensitivity to run data assimilation and the prior ranges were cited from published papers for the same or similar ecosystems (Table 1). The errors between each observation data and model simulation result independently follow normal distribution with a zero mean, so the likelihood function is represented by

$$p(Z|\theta) \propto \exp \left\{ - \sum_{t \in Z_i} \frac{[Z_i(t) - X(t)]^2}{2\sigma_i^2(t)} \right\} \quad (19)$$

where $Z_i(t)$ is the only observation stream at time t , $X(t)$ is the simulated corresponding variable, and $\sigma_i(t)$ is the standard deviation of observation set.

The Markov chain Monte Carlo technique was used for posterior probability distribution of parameters sampling with adaptive Metropolis-Hastings (M-H) algorithm. A new vector of candidate parameters was repeatedly proposed based on the accepted parameters in the previous steps by a normal distribution. The new set

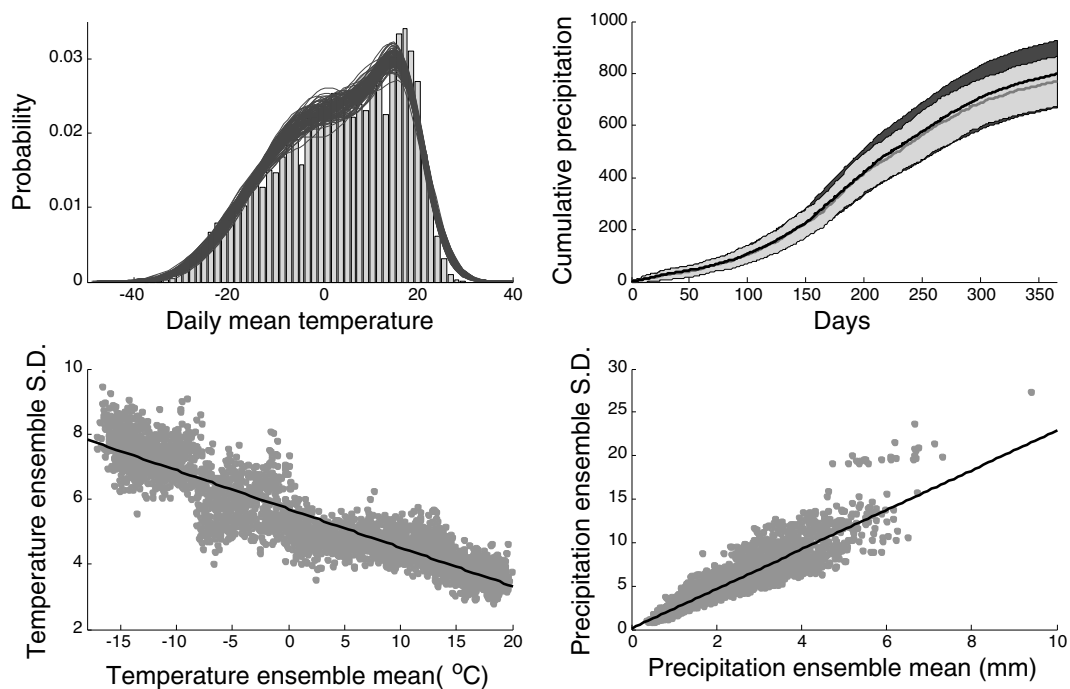


Figure 2. Historical climate from the USDA MEF site during 1961–2014 and stochastic weather generation for 2015–2024. (top left) Probability density distribution of daily mean temperature (gray bar graph represents historical observation data, and black curves represent ensemble of predicted future temperatures). (top right) Cumulative precipitation within a year (curve and shaded areas represent mean and standard deviation, respectively; gray is historical observation data, and black is future predictions). Standard deviations versus means for daily (bottom left) air temperature and (bottom right) precipitation. Credits from Jiang Jiang.

of parameter values would be accepted either by reducing the sum of standard deviation from observation and model or being randomly accepted with a probability of 0.05. We ran four chains of 50,000 simulations with an acceptance rate around 30% and used the Gelman-Rubin statistic (Gelman & Rubin, 1992; Xu et al., 2006) to check the convergence of sampling chains. Only the second half of accepted parameter values were used for posterior analysis considering the burn-in period in the first half.

2.5. Stochastic Weather Generation

We generated 300 sets of 10 year environmental variables (2016–2024). Daily air temperature and precipitation were stochastically generated based on historical data from 1961 to 2014 at the MEF South Meteorological station using a vector autoregressive model (VAR, Figure 2).

To match the model time step, hourly precipitation was obtained by evenly distributing daily precipitation for each hour, hourly air temperature was interpolated from daily maximum and minimum, and soil temperature was calculated from air temperature based on linear regression between soil temperature and air temperature at S1 Bog from 2011 to 2014. The generated air temperature generally follows the same distribution as the historical temperature (Figure 2, top left). The standard deviation of generated temperature decreases with increasing daily mean temperature (Figure 2, bottom left), which indicates a larger uncertainty of generated future temperature in winter than in summer. Future prediction of precipitation is similar to the historical precipitation with slightly higher variation (Figure 2, right column). We increased both the air temperature and soil temperature by 2.25°C, 4.5°C, 6.75°C, and 9°C and the atmospheric CO₂ value by 500 ppm to simulate CH₄ emission in different scenarios manipulated at the SPRUCE site.

3. Results

3.1. Parameters Constrained by Data Assimilation in TECO_SPRUCE_ME

The model output was sensitive to five out of nine tested parameters in the growing season (Figure 3): potential ratio of anaerobically mineralized carbon released as CH₄ (r_{me}), Q_{10} for CH₄ production (Q_{10_pro}),

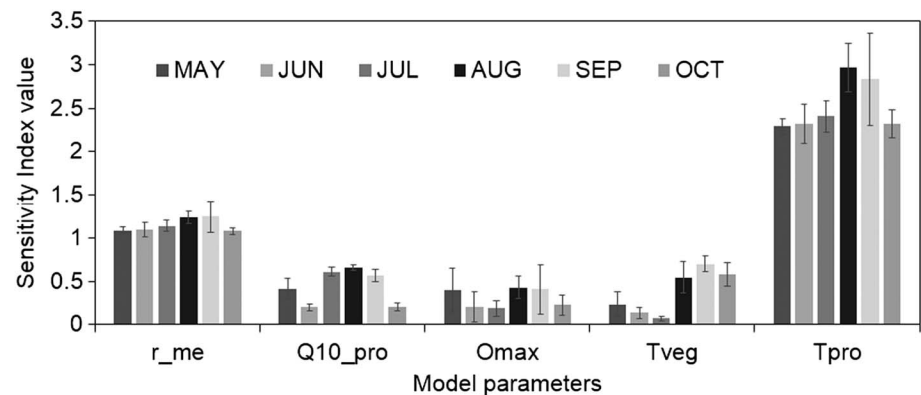


Figure 3. Sensitivity index for the most influential parameters for CH_4 fluxes during the growing season (4 year average of 2011–2014) in May, June, July, August, September, and October. The error bar denotes standard deviation.

maximum oxidation rate (O_{max}), ability of plant-mediated transportation decided by species composition and plant density (T_{veg}), and optimum temperature for CH_4 production (T_{opt_pro}) with sensitivity index values higher than 0.2. T_{opt_pro} and r_{me} had the highest sensitivity index values throughout the growing season (sensitivity class >1.00 , very high), suggesting the importance of temperature and soil substrate in methanogenesis to methane emission. Q_{10_pro} , O_{max} , and T_{veg} rank in the second class of sensitivity, and the sensitivity index values varied across growing season. Q_{10_pro} had the lowest value of sensitivity index in July and October (around 0.2). O_{max} and T_{veg} had the highest sensitivity index value in peak growing season (August, September, and October, around 0.5), suggesting the importance of plant root transportation and oxidation on methane emission in response to environmental change.

There are strong interaction effects among r_{me} , Q_{10_pro} , and T_{opt_pro} as these parameters are multiplied in the same equation for methane production. We settled a reasonable value of T_{opt_pro} to 20.0 based on published incubation results (Wilson et al., 2016) and the values cited in other modeling papers (Zhu et al., 2014; Zhuang et al., 2004), so as to better constrain the other parameter values using data assimilation. Two out of four parameters put into data assimilation were constrained including r_{me} and Q_{10_pro} (Figure 4). Histograms of parameter show that the distribution of r_{me} is well constrained with a unimodal shape and the distribution of Q_{10_pro} is edge hitting with a marginal distribution upward (Figures 4a and 4b). T_{veg} and O_{max} have the largest variability and wide, slightly domed distributions (Figures 4c and 4d), which may have resulted from a limited number of observation data points and large variation in the CH_4 emission measurements.

3.2. Simulation, Validation, and Forecast in Ambient Condition

Our simulated CH_4 flux well captured the general seasonal changes in the CH_4 emission observed by the large collar chamber (Figure 5). The mean annual methane efflux from 2011 to 2014 was $16.5 \pm 2.0 \text{ g C m}^{-2} \text{ yr}^{-1}$. We applied observational data from January 2015 to August 2016 for model forecasting validation (Figure 5), with the parameters constrained in the data assimilation stage using the observational data from 2011 to 2014. During the forecasted period of 2015–2016, the seasonal changes of methane emission are well captured by the model (Figure 5). To better show the seasonal variation, we picked the first year in the simulation (2011) and plotted daily variation of water table (simulated), surface soil temperature (measured), and methane emission (simulated) in Figures 5a–5c. In general, the highest water table conditions occurred in late spring (May) and middle to late summer (July to August), while lower levels occurred in middle spring (April), early summer (June), and end of July. Before the month of July when the daily mean soil temperature was below 10°C , methane emission was restricted by temperature. During the peak growing season the decrease of methane emission was mainly driven by low water level. When the water table was at or above the soil surface, CH_4 emissions were more sensitive to variability in soil temperature. During the period from September 2016 to December 2024, the variation amplitudes of CH_4 emissions were relatively higher due to the statistically generated weather forcing data, while the general seasonal pattern remained the same with that from January 2011 to August 2016 (Figure 5).

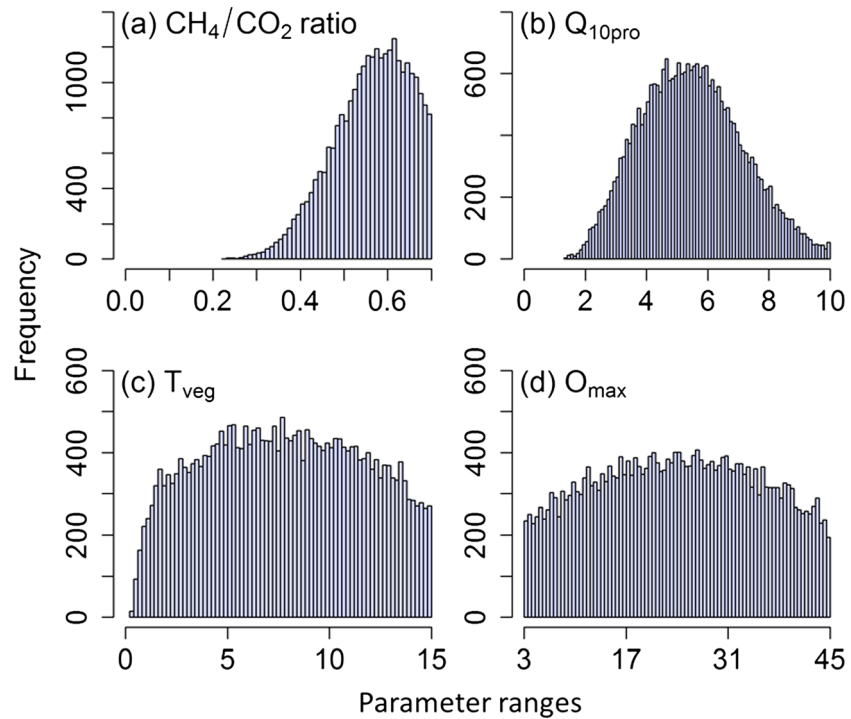


Figure 4. Posterior distributions of parameters of 50,000 samples from M-H simulation. (a) Potential ratio of anaerobically mineralized carbon released as CH₄, (b) Q₁₀ for CH₄ production, (c) maximum oxidation rate, and (d) factor of transport ability at plant community level.

3.3. Responses of Water Table and CH₄ Emission to Warming and Elevated CO₂

Our modeling results showed no significant changes of water table elevation in response to whole-ecosystem warming treatment. By using constrained parameter values, we were able to simulate CH₄ emission in the bog and found that warming significantly increased methane emission by 1.5, 2.1, 3.0, and 4.2

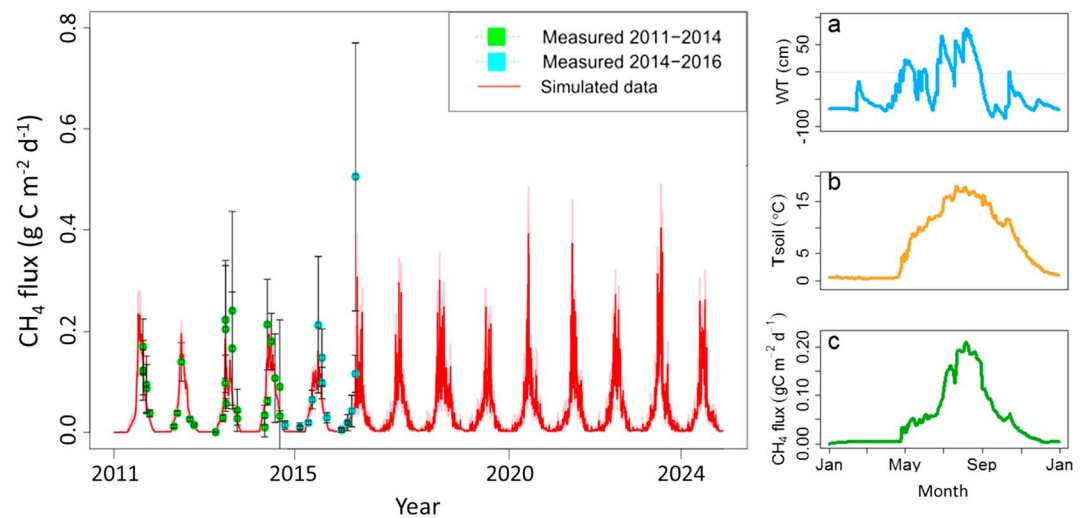


Figure 5. Forecasting of CH₄ emission dynamics based on stochastically generated weather forcing data. Green dots refer to observations from 2011 to 2014 which were used for data assimilation. Blue dots indicate observations from 2015 to 2016 which were used for model validation, and error bars indicate the standard deviation of each observation. Red line is simulated mean methane emission. The shading area corresponds to 1 standard deviation based on 500 randomly chosen model simulations with parameters drawn from the posterior distribution. (a–c) The 2011 daily variation of water table, surface soil temperature, and methane emission.

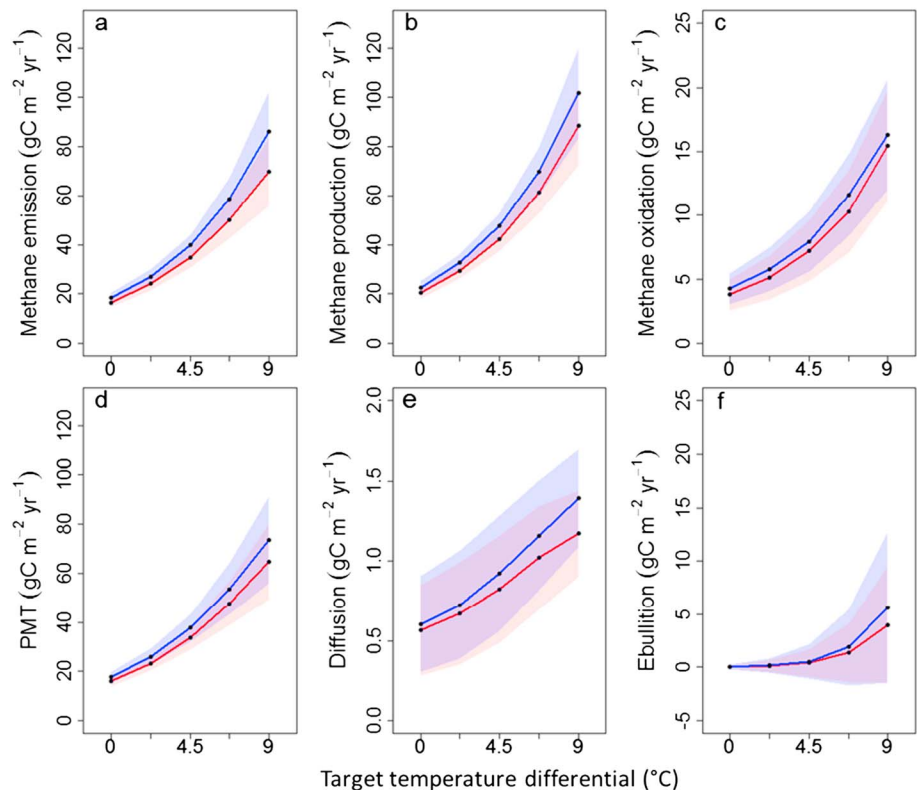


Figure 6. Responses of annual CH_4 emission to warming and elevated CO_2 (eCO_2). Red lines indicate CH_4 fluxes under warming treatments and 380 ppm CO_2 , blue lines indicate CH_4 fluxes under warming treatments and 880 ppm CO_2 . X axes indicate the warming treatments of +0°C, +2.25°C, +4.5°C, +6.75°C, and +9°C above ambient level. Shaded area corresponds to mean ± 1 standard deviation based on 500 randomly chosen model simulations with parameters drawn from the posterior distribution.

times under +2.25°C, +4.5°C, +6.75°C, and +9°C, respectively (Figure 6a), while elevated CO_2 only had a small stimulating effect ($\sim 10.4\%$ – 28.6%) on methane emission (Figure 6a). Both CH_4 production and oxidation increased by about 4 times above ambient level with 9°C warming with enlarged uncertainties especially in the growing seasons (Figures 6b, 6c, 8b, 8c, 9b, and 9c). Plant-mediated transport is the major pathway of CH_4 emission which increased by ~ 4 times above the ambient level under 9°C warming (Figures 6d, 8a, 8d–8f, 9a, and 8d–8f); however, its relative contribution to methane emission decreased from 96% to 92% due to the increased ebullition (Figure 7). At the same time, in ambient conditions the uncertainty of plant transported began to increase in early August (Figure 8d), but the starting point moved up to late June under 9°C warming (Figure 9d). The absolute value of uncertainty was 10 times the value without treatment. In ambient conditions, ebullition contributed 0.13% ($0.02 \text{ g C m}^{-2} \text{ yr}^{-1}$) of total emission, while under 9°C warming the total amount of bubbles released into the atmosphere increased to 5.7% ($4.0 \text{ g C m}^{-2} \text{ yr}^{-1}$) of total emission (Figure 7). The uncertainty in plant-mediated transportation and ebullition both increased under warming (Figures 6d and 6f), while the uncertainty in diffusion did not change much (Figure 6e). The simulated results showed that diffusion contributed 3.4% ($0.57 \text{ g C m}^{-2} \text{ yr}^{-1}$) of total emission, and it decreased to 1.7% ($1.17 \text{ g C m}^{-2} \text{ yr}^{-1}$) of total emission under 9°C warming (Figure 7).

4. Discussion

4.1. Model Performance in Reducing Uncertainties

Data-model fusion reduced the uncertainty of methane emission estimation by constraining the CH_4 and CO_2 ratio and temperature sensitivity for CH_4 production. In our model, with 30 data points of daily methane emission from 2011 to 2014, two out of four parameters were well constrained or marginally edge hitting. Gill et al. (2017) estimated the mean value of CH_4 flux Q_{10} to be 5.63 (2.92–10.52 with 95% confidence interval) using a

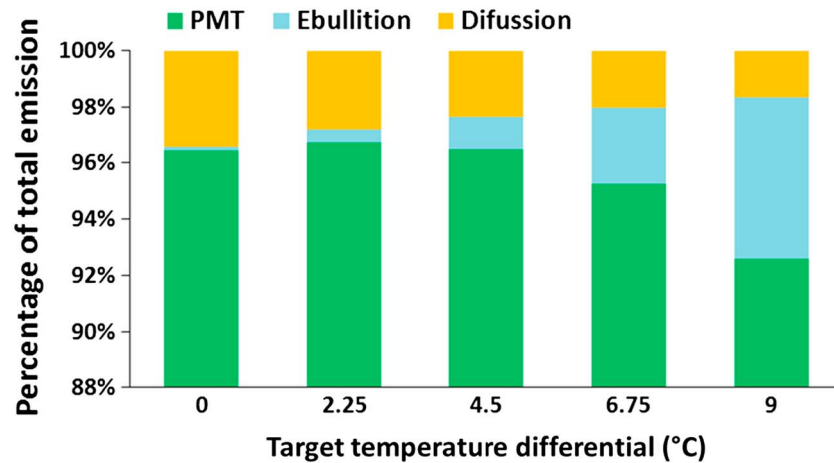


Figure 7. Simulated percentage of total emission in different pathways (plant-mediated transportation (PMT), ebullition, and diffusion) using the mean value from 100 accepted parameter sets.

linearized Q_{10} function (Humphreys et al., 2005) at the same study site during the 2015 growing season. Our constrained Q_{10} range was 2.34–6.33 with 95% confidence interval, which overlaps with but has a narrower range than that estimate by Gill et al. (2017).

Equifinality and identifiability are the symptoms of using only one data stream to constrain multiple parameters in a model (Braswell et al., 2005; Keenan et al., 2011; Luo et al., 2009; Wang et al., 2001). Oikawa et al. (2016) used 1 year of half hourly eddy covariance CH_4 emission data and constrained three parameters in the CH_4 module of PEPRMT-DAMM model. Although the posterior ranges of two out of four key parameters in TECO_SPRUCE_ME have been constrained and thus the uncertainty has been reduced, there is still some uncertainty due to the unconstrained parameter O_{max} and lack of observation data available to constrain the other three parameters to a smaller range. More parameters could be constrained with more measurement data available, such as more data points in an extended length of time, as well as CH_4 concentration and CH_4 oxidation in different soil layers.

Our simulated CH_4 flux captured the general seasonal changes in CH_4 emissions observed by the large collar chamber (Figure 5). Seasonal variations in wetland CH_4 fluxes are mostly determined by temporal changes in peatland water volume and soil temperature (Gedney, Cox, & Huntingford, 2004; Walter, Heimann, & Matthews, 2001). We found that soil temperature was the restricting factor when below 10°C, while during the peak growing season the decrease of CH_4 emission was mainly determined by the lower water table (Figure 5). CH_4 emission was more sensitive to variability in soil temperature during the wet time when the water table was at or above the soil surface.

For the purpose of reducing simulation uncertainties by using data assimilation to constrain the key parameters value, we did not fully incorporate all the processes and scalars described in other studies, such as the effect of competition between processes (Riley et al., 2011), pH, and redox potential (Cao et al., 1998; Segers & Kengen, 1998; Zhu et al., 2014). There are always trade-offs between the desire to include all the mechanisms assumed to be important and (1) reducing those uncertainties from assumed model structure, (2) lack of prior knowledge of nonkey parameter values, and (3) the computational cost when applying data assimilation.

4.2. Warming and eCO₂ Effects on CH₄ Emission

By using constrained parameter values, we were able to simulate CH_4 emission in the bog wetland and found an exponential increase under warming (Figure 6a). Wilson et al. (2016) fitted seasonal flux measurements against the average temperature from 1 m to 2 m below the hollow surface and also found an exponential increase in CH_4 emission using chamber flux measurements, also as part of SPRUCE. Methane emissions were most responsive to warming during the peak growing season, which could explain greater uncertainty in growing season in response to warming simulated by the model (Figure 8a and 9a). We found that elevated CO_2 had a small stimulating effect (~10.4%–28.6%) on methane emission (Figure 6a), due to increased

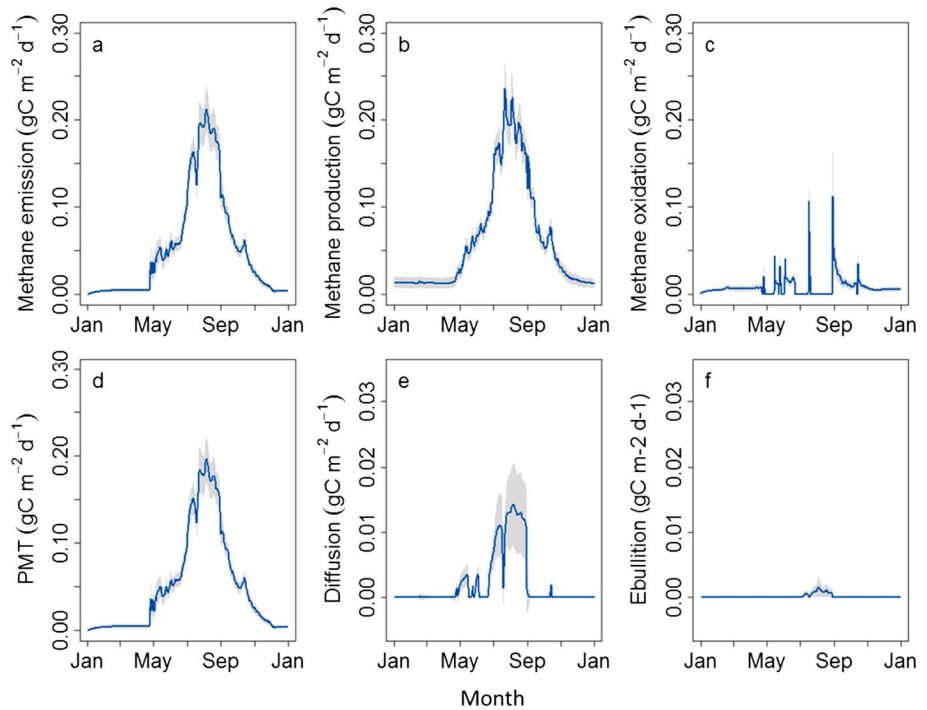


Figure 8. Simulated seasonal methane fluxes variation in 2011 under ambient condition. Blue lines indicate CH₄ fluxes under ambient temperature and 380 ppm CO₂. Shading areas correspond to mean ± 1 standard deviation based on 500 randomly chosen model simulations with parameters drawn from the posterior distribution.

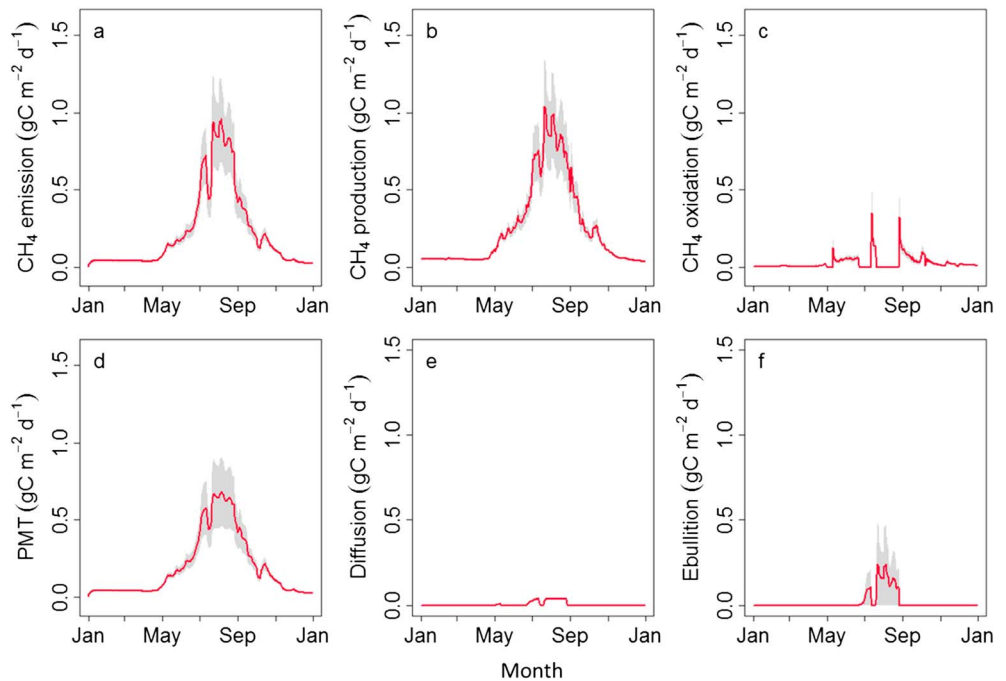


Figure 9. Simulated seasonal methane fluxes variation in 2011 under +9°C warming condition. Red lines indicate CH₄ fluxes under +9°C warming and 380 ppm CO₂. Shaded areas correspond to mean ± 1 standard deviation based on 500 randomly chosen model simulations with parameters drawn from the posterior distribution.

substrate supply for methanogenesis. Elevated CO₂ has stimulating effects on soil respiration in TECO model through increased photosynthesis and thus increased substrate supply for mineralization (Shi et al., 2015).

We compared our results with other modeling and experimental work. The Wetland and Wetland CH₄ Inter Comparison of Models Project (WETCHIMP) simulated the change in global methane emission in response to temperature increase (+3.7°C) and elevated CO₂ (step increase from ~300 to 857 ppm) using 10 global models (Melton et al., 2013). An ~160% increase in global CH₄ flux was found in ORCHIDEE model with the largest sensitivity to increased CO₂; other model results showed an increase of global CH₄ emission from 73.2% ±49.1% to 55.4% ± 25.5%. Our results showed that elevated CO₂ treatments stimulated methane emission by 10.4%–23.6% per unit at site level. The difference may be attributable to their expectation of an ~13% increase of global wetland areal extent under the elevated CO₂ scenarios. Furthermore, different wetland types, such as bogs and fens, may respond differently to CO₂ enrichment (Boardman et al., 2011).

Our findings of increased methane emission with CO₂ enrichment are also consistent with experiments. Methane emissions in natural wetlands and mesocosms generally have increased with exposure to elevated atmospheric CO₂ (Meronigal & Schlesinger, 1997; Saarnio et al., 2003; Saarnio & Silvola, 1999). In a meta-analysis study, Van Groenigen, Osenberg, and Hungate (2011) reported an increase of methane emission from natural wetlands of 13.2% per area for an atmospheric CO₂ concentration increase from 473 to 780 ppm. In an incubation study, Kang, Freeman, and Ashendon (2001) found no significant differences in CH₄ emission regardless a significantly higher biomass in a fen peatland.

Our results showed a much stronger response of methane emission (30%, 100%, 275%, and 400% under 2.25, 4.5, 6.75, 9°C warming) mainly due to no significant changes in water table elevation in response to the whole-ecosystem warming treatment in this area, which was in agreement with observed water table depth during the deep peat warming period (Wilson et al., 2016). The same pattern of water elevation under warming was also projected by CLM model at the same study site (Shi et al., 2015). Zhu et al. (2011) estimated CH₄ emission in Northern Eurasia with the Terrestrial Ecosystem Model (TEM) model for the period 1971–2100 (annual mean soil temperature gradually increased by ~6°C, and annual precipitation gradually increased by 30%). They found that the water table dropped due to the increased soil temperature, which diminished water table rising after additional rainfall. Using various data sets on wetland extent, regional methane emission increased by 6–51%. Results from WETCHIMP showed a slight, nonsignificant decline in global methane emission with warming (+3.7°C), due to a moderate decline in wetland area (Melton et al., 2013). Institute of Atmospheric Physics RAS global climate model (IAP) is the only model showing a large increase in CH₄ emissions, because it does not simulate increased evaporation under warmer surface air temperature or an effect decreasing wetland area with increased evaporation. Wetlands from different regions may also have differential responses to elevated temperature. In warm regions, methane production may decrease if elevated temperature causes downregulation of photosynthesis and henceforth production of substrate for methane production (Melton et al., 2013). Bohn et al. (2007) used the variable infiltration capacity macroscale hydrological model (VIC) biosphere-energy-transfer-hydrology terrestrial ecosystem model (BETHY) model and simulated methane emission in western Siberia. They found increased methane production with higher temperature alone (0–5°C), but overall, shrinking of wetland area resulted in a net reduction in methane emissions.

Our simulation results showed that the total CH₄ production increased by 4 times under 9°C warming, while the heterotrophic respiration has only increased by ~25% in comparison to ambient temperatures. That large contrast between methane production and respiration implies a higher temperature dependence of methanogenesis than respiration. A similar result was also found at the same site in an incubation study (Wilson et al., 2016), where they found a positive correlation between CH₄:CO₂ emission ratio and increased temperature. Consistently higher temperature dependence in methanogenesis was also found across the ecosystem (field flux measurement), community (CH₄ incubation), and species levels (pure culture) (Yvon-Durocher et al., 2014).

We did not find differential responses of CH₄ emission in different layers, while the incubation study by Wilson et al. (2016) showed that the increased CH₄ emission was largely driven by surface peat (25 cm) warming by measuring CH₄ production in different layers (25 cm, 75 cm, 100 cm, 150 cm, and 200 cm). The Q₁₀ for CH₄ production (Q_{10_pro}) may vary in different soil layers, and this parameter value is important when estimating CH₄ emission under warming. Different Q₁₀ values for surface and catotelm soil may be needed in

methane models. One possible solution is to add o-alkyl carbon (C) content as a function of basal Q_{10} into the equation, because the lack of reactivity from deep peat to warming was speculated to result from low o-alkyl C (Leifeld, Steffens, & Galego-Sala, 2012; Tfaily et al., 2014; Wilson et al., 2016).

In order to eliminate the interaction effect between r_{me} , Q_{10_pro} , and T_{opt_pro} when constraining their values, we set one of the key parameters T_{opt_pro} (reference temperature for methanogenesis) to 20°C in this ecosystem. A wide range of T_{opt_pro} values (−5.5–25°C) have been used in methane models for various ecosystems. Even in one single ecosystem type, for example, the boreal forest, the value used in different models, varies from 10°C (Zhuang et al., 2004) to 25°C (Zhu et al., 2014). As T_{opt_pro} is an extremely sensitive parameter in TECO_SPRUCE_ME model, we carefully estimated the value according to the temperature response of CH₄ production from surface peat samples incubated within 1°C of in situ temperatures from the same study site (Wilson et al., 2016). In biogeochemical models all the reference temperatures for foliar respiration (Wythers et al., 2005), soil respiration (Luo et al., 2001), and root respiration (Atkin, Edwards, & Loveys, 2000) were set to constant values, even when the acclimation effect on Q_{10} and specific reaction rate at a reference temperature were considered. This method was chosen partially because the reference temperature is an intrinsic biological term which is stable under a certain combination of organisms, for example, the structure of the microbial community, and the concentration and quality of soil organic matter. On the other hand, the potential change in reference temperature due the change in depth and substrate supply could be reflected by the change in Q_{10} .

4.3. Differential Responses of CH₄ Emission Pathways to Warming and eCO₂

Removal of the vascular plants (*Eriophorum vaginatum*) in a Swedish boreal peatland decreased the seasonal CH₄ flux by 55%–85% (Waddington, Roulet, & Swanson, 1996). Wania et al. (2010) estimated the contribution of plant-mediated transport to be 67.8%–84.5% across different sites using the LPJ-WHyMe model. In Arctic tundra, plant-mediated transport represented 92%–98% of the net emission measured by static chamber (clipping 100%, 50%, and 0% of the phytomass quantity within the sample chamber (Morrissey & Livingston, 1992)). Plant-mediated transport was 92–96.5% of total emission at our study site. The contribution of plant-mediated CH₄ efflux to total emission may be underestimated in some biogeochemical models where trees, forbs, and shrubs were not included either because of the low Net Primary Production (NPP) contribution or assumptions about the capacity of these various plant types to mediate gas transport (Wania et al., 2010; Zhuang et al., 2004). Lignified or suberized plants, such as trees, are considered incapable of transporting CH₄. However, in the past 10 years some studies have detected considerable CH₄ efflux from stems (Carmichael et al., 2014; Pitz & Megonigal, 2017; Terazawa et al., 2007). Trees in boreal forests have been found to emit methane from both stems and shoots (Machacova et al., 2016). Tree-mediated CH₄ emissions contribute up to 27% of seasonal ecosystem CH₄ flux in a temperate forested wetland (Pangala et al., 2015). In the TECO model, roots were not separated into tree, shrub, and grass but we used a scaler T_{veg} , a parameter that was determined by type and plant density. This parameter represents the ability of plant to transport CH₄ at the community level. Plant-mediated transport of CH₄ from deep soil layers may have been overestimated as the trees and shrubs may transport less CH₄ than grasses and sedges. More data on the relative effects of different plant functional types on CH₄ transport are needed. For the long-term projections, vegetation change should be considered as CH₄ emission is sensitive to T_{veg} . The constant value used for T_{veg} in global methane emission models (Riley et al., 2011; Zhang et al., 2002; Zhu et al., 2014; Zhuang et al., 2004) may bias for CH₄ emission estimates.

Diffusion accounts for ~5% on average in south Florida wetlands (Barber, Burke, & Sackett, 1988). Ebullition accounts for 10%–60% of the emission (Chanton, Martens, & Kelley, 1989; Tokida et al., 2007). At the SPRUCE site, Gill et al. (2017) did chamber measurements but used 30 cm diameter collars to measure methane emissions at a smaller community level. Trees, shrubs, and plants with well-developed aerenchyma tissues, such as *Eriophorum spissum*, were excluded at this measurement scale. They estimated 2015 growing season ebullition fluxes to be 1% of total CH₄ flux measurements averaged from different warming treatments by considering CH₄ fluxes >2 standard deviations of the median as products of CH₄ ebullition. We estimated that diffusion and ebullition accounted for 3.4% and 0.1%, respectively. We found that CH₄ production rate drives the overall pattern of CH₄ emission (Figures 7a and 7b). Due to a higher CH₄ concentration in soil layers, the relative contribution of ebullition increased from 0.13% at the control to 5.7% at the 9°C warming,

given the fact that any “excess” CH₄ is immediately released into the atmosphere when water table is above the soil surface. Although the absolute value of diffusion fluxes increased from 0.57 at the control to 1.17 g C m⁻² yr⁻¹ at the 9°C warming, the relative contribution of diffusion decreased to 1.7% from 3.4%. Our model simulation of ebullition matched the observational data, which implied that model-data fusion differentiates responses of plant-mediated transportation, diffusion, and ebullition to climate change. The uncertainty in plant-mediated transportation and ebullition increased under warming and contributed to the overall change of uncertainty in emission.

4.4. Future Studies

Existing methane models use a constant value of ecosystem-specific parameters such as Q_{10} for CH₄ production (Q_{10_pro}) and potential ratio of anaerobically mineralized carbon released as CH₄ (r_me). Under long-term warming conditions, however, ecosystem acclimation to temperature may result in a change in Q_{10} (Gill et al., 2017; Wythers et al., 2005) and r_me . Through our data-model fusion framework, the long-term change in parameter values may be detected by combining the long-term CH₄ emission measurement data and more data sets coming out such as CH₄ concentration in different layers and CH₄ oxidation rate.

5. Conclusions

We developed a methane module, which included processes of methane production, methane oxidation, plant-mediated methane transportation, diffusion through different layers, and ebullition, together with water table dynamics. The methane module was integrated into the Terrestrial ECOSystem (TECO) model. After constraining the parameters with multiple years of methane emission data in a northern Minnesota peatland, we used the model to forecast CH₄ emission until 2024 under five warming and two elevated CO₂ treatments. We found that 9°C warming significantly increased methane emission by 4 times above ambient conditions and elevated CO₂ stimulated methane emission by 10.4%–23.6%. The uncertainty in plant-mediated transportation and ebullition increased under warming and contributed to the overall change of uncertainty in CH₄ emission estimates. The model-data fusion approach used in this study enabled parameter estimation and uncertainty quantification for forecasting methane fluxes. As additional data for warming and elevated CO₂ treatments become available, the data-model fusion may help estimate parameter changes as ecosystems acclimate over time. The sensitivity of T_{opt_pro} and T_{veg} suggested that these could be key parameters to be measured in the field so as to reduce uncertainties in process-based models. Furthermore, the larger warming potential of CH₄ may result in a more positive feedback of global warming in terrestrial ecosystems.

Acknowledgments

We thank Russell Doughty for his English language editing of this manuscript. Xingjie Lu and Junyi Liang offered technical help on coding and debugging. This work was primarily funded by subcontract 4000144122 from Oak Ridge National Laboratory (ORNL) to the University of Oklahoma. Oak Ridge National Laboratory is managed by UT-Battelle, LLC, for the U.S. Department of Energy under contract DE-AC05-00OR22725. Research in Yiqi Luo’s EcoLab was also financially supported by U.S. DOE grants DE-SC0008270 and DE-SC00114085 and U.S. National Science Foundation (NSF) grants EF 1137293 and OIA-1301789. All data sets from this study are available upon request. Relevant measurements were obtained from the SPRUCE Webpage (<http://mnspruce.ornl.gov/>), the archival ftp site (<ftp://sprucedata.ornl.gov/>), or from the USDA Forest Service. Data of the TECO_SPRUCE_ME model are available at <http://dx.doi.org/10.3334/CDIAC/spruce.046>. This manuscript has been co-authored by a Federal employee. The United States Government retains, and the publisher, by accepting the article for publication, acknowledges that the United States Government retains a nonexclusive, paid-up, irrevocable, worldwide license to publish or reproduce the published form of this manuscript, or allow others to do so, for United States Government purposes.

References

- Atkin, O. K., Edwards, E. J., & Loveys, B. R. (2000). Response of root respiration to changes in temperature and its relevance to global warming. *The New Phytologist*, 147(1), 141–154. <https://doi.org/10.1046/j.1469-8137.2000.00683.x>
- Barber, T. R., Burke, R. A., & Sackett, W. M. (1988). Diffusive flux of methane from warm wetlands. *Global Biogeochemical Cycles*, 2(4), 411–425. <https://doi.org/10.1029/GB002i004p00411>
- Bartlett, K. B., Crill, P. M., Bonassi, J. A., Richey, J. E., & Harris, R. C. (1990). Methane flux from the Amazon River floodplain: Emissions during rising water. *Journal of Geophysical Research*, 95(D10), 16,773–16,788. <https://doi.org/10.1029/JD095iD10p16773>
- Bender, M., & Conrad, R. (1992). Kinetics of CH₄ oxidation in oxic soils exposed to ambient air or high CH₄ mixing ratios. *FEMS Microbiology Letters*, 101(4), 261–270. <https://doi.org/10.1111/j.1574-6968.1992.tb05783.x>
- Boardman, C. P., Gauci, V., Watson, J. S., Blake, S., & Beerling, D. J. (2011). Contrasting wetland CH₄ emission responses to simulated glacial atmospheric CO₂ in temperate bogs and fens. *New Phytologist*, 192(4), 898–911. <https://doi.org/10.1111/j.1469-8137.2011.03849.x>
- Bohn, T. J., Lettenmaier, D. P., Sathulur, K., Bowling, L. C., Podest, E., McDonald, K. C., & Friborg, T. (2007). Methane emissions from western Siberian wetlands: Heterogeneity and sensitivity to climate change. *Environmental Research Letters*, 2(4), 045015. <https://doi.org/10.1088/1748-9326/2/4/045015>
- Braswell, B. H., Sacks, W. J., Linder, E., & Schimel, D. S. (2005). Estimating diurnal to annual ecosystem parameters by synthesis of a carbon flux model with eddy covariance net ecosystem exchange observations. *Global Change Biology*, 11(2), 335–355. <https://doi.org/10.1111/j.1365-2486.2005.00897.x>
- Bridgman, S. D., Cadillo-Quiroz, H., Keller, J. K., & Zhuang, Q. (2013). Methane emissions from wetlands: Biogeochemical, microbial, and modeling perspectives from local to global scales. *Global Change Biology*, 19(5), 1325–1346. <https://doi.org/10.1111/gcb.12131>
- Bridgman, S. D., Megonigal, J. P., Keller, J. K., Bliss, N. B., & Trettin, C. (2006). The carbon balance of North American wetlands. *Wetlands*, 26(4), 889–916. [https://doi.org/10.1672/0277-5212\(2006\)26%5B889:TCBONA%5D2.0.CO;2](https://doi.org/10.1672/0277-5212(2006)26%5B889:TCBONA%5D2.0.CO;2)
- Bubier, J. L., Moore, T. R., Bellisario, L., Comer, N. T., & Crill, P. M. (1995). Ecological controls on methane emissions from a Northern Peatland Complex in the zone of discontinuous permafrost, Manitoba, Canada. *Global Biogeochemical Cycles*, 9(4), 455–470. <https://doi.org/10.1029/95GB02379>
- Cao, M., Dent, J. B., & Heal, O. W. (1995). Modeling methane emissions from rice paddies. *Global Biogeochemical Cycles*, 9(2), 183–195. <https://doi.org/10.1029/94GB03231>

- Cao, M., Gregson, K., & Marshall, S. (1998). Global methane emission from wetlands and its sensitivity to climate change. *Atmospheric Environment*, 32(19), 3293–3299. [https://doi.org/10.1016/S1352-2310\(98\)00105-8](https://doi.org/10.1016/S1352-2310(98)00105-8)
- Cao, M., Marshall, S., & Gregson, K. (1996). Global carbon exchange and methane emissions from natural wetlands: Application of a process-based model. *Journal of Geophysical Research*, 101(D9), 14,399–14,414. <https://doi.org/10.1029/96JD00219>
- Carmichael, M. J., Bernhardt, E. S., Bräuer, S. L., & Smith, W. K. (2014). The role of vegetation in methane flux to the atmosphere: Should vegetation be included as a distinct category in the global methane budget? *Biogeochemistry*, 119(1-3), 1–24. <https://doi.org/10.1007/s10533-014-9974-1>
- Chanton, J. P., & Dacey, J. W. H. (1991). Effects of vegetation on methane flux, reservoirs, and carbon isotopic composition. In T. D. Sharkey, E. A. Holland, & H. A. Mooney (Eds.), *Trace Gas Emissions by Plants* (pp. 65–92). San Diego, CA: Academic Press. <https://doi.org/10.1016/B978-0-12-639010-0.50008-X>
- Chanton, J. P., Martens, C. S., & Kelley, C. A. (1989). Gas transport from methane-saturated, tidal freshwater and wetland sediments. *Limnology and Oceanography*, 34(5), 807–819. <https://doi.org/10.4319/lo.1989.34.5.0807>
- Conrad, R. (1999). Contribution of hydrogen to methane production and control of hydrogen concentrations in methanogenic soils and sediments. *FEMS Microbiology Ecology*, 28(3), 193–202. <https://doi.org/10.1111/j.1574-6941.1999.tb00575.x>
- Dise, N. B., Gorham, E., & Verry, E. S. (1993). Environmental factors controlling methane emissions from peatlands in northern Minnesota. *Journal of Geophysical Research*, 98(D6), 10,583–10,594. <https://doi.org/10.1029/93JD00160>
- Fiedler, S., & Sommer, M. (2000). Methane emissions, groundwater levels and redox potentials of common wetland soils in a temperate-humid climate. *Global Biogeochemical Cycles*, 14(4), 1081–1093. <https://doi.org/10.1029/1999GB001255>
- Forster, P., Ramaswamy, V., Artaxo, P., Bernsten, T., Betts, R., Fahey, D. W., ... Van Dorland, R. (2007). Changes in atmospheric constituents and in radiative forcing. In S. Solomon, et al. (Eds.), *Climate change 2007: The physical science basis. Contribution of working group I to the fourth assessment report of the intergovernmental panel on climate change*. Cambridge, United Kingdom and New York: Cambridge University Press.
- Frolking, S., & Crill, P. (1994). Climate controls on temporal variability of methane flux from a poor fen in southeastern New Hampshire: Measurement and modeling. *Global Biogeochemical Cycles*, 8(4), 385–397. <https://doi.org/10.1029/94GB01839>
- Frolking, S., Roulet, N., & Fuglested, J. (2006). How northern peatlands influence the Earth's radiative budget: Sustained methane emission versus sustained carbon sequestration. *Journal of Geophysical Research*, 111, G01008. <https://doi.org/10.1029/2005JG000091>
- Gedney, N., Cox, P. M., & Huntingford, C. (2004). Climate feedback from wetland methane emissions. *Geophysical Research Letters*, 31, L20503. <https://doi.org/10.1029/2004GL020919>
- Gelman, A., & Rubin, D. B. (1992). Inference from iterative simulation using multiple sequences. *Statistical Science*, 7(4), 457–472. <https://doi.org/10.1214/ss/1177011136>
- Gerard, G., & Chanton, J. (1993). Quantification of methane oxidation in the rhizosphere of emergent aquatic macrophytes: Defining upper limits. *Biogeochemistry*, 23(2), 79–97. <https://doi.org/10.1007/BF00000444>
- Gill, A. L., Giasson, M. A., Yu, R., & Finzi, A. C. (2017). Deep peat warming increases surface methane and carbon dioxide emissions in a black spruce dominated ombrotrophic bog. *Global Change Biology*, 1–14. <https://doi.org/10.1111/gcb.13806>
- Granberg, G., Grip, H., Löfvenius, M. O., Sundh, I., Svensson, B. H., & Nilsson, M. (1999). A simple model for simulation of water content, soil frost, and soil temperatures in boreal mixed mires. *Water Resources Research*, 35(12), 3771–3782. <https://doi.org/10.1029/1999WR900216>
- Granberg, G., Sundh, I., Svensson, B. H., & Nilsson, M. (2001). Effects of temperature, and nitrogen and sulfur deposition, on methane emission from a boreal mire. *Ecology*, 82(7), 1982–1998. <https://doi.org/10.2307/2680063>
- Hanson, P. J., Gill, A. L., Xu, X., Phillips, J. R., Weston, D. J., Kolka, R. K., ... Hook, L. A. (2016). Intermediate-scale community-level flux of CO₂ and CH₄ in a Minnesota peatland: Putting the SPRUCE project in a global context. *Biogeochemistry*, 129(3), 255–272. <https://doi.org/10.1007/s10533-016-0230-8>
- Hanson, P. J., Phillips, J. R., Riggs, J. S., & Nettles, W. R. (2017). *SPRUCE Large-Collar in Situ CO₂ and CH₄ Flux Data for the SPRUCE Experimental Plots: Whole-Ecosystem-Warming*. Oak Ridge, TN: Carbon Dioxide Information Analysis Center, Oak Ridge National Laboratory, U.S. Department of Energy. <https://doi.org/10.3334/CDIAC/spruce.034>
- Hanson, P. J., Riggs, J. S., Nettles, W. R., Phillips, J. R., Krassovski, M. B., Hook, L. A., ... Barbier, C. (2016). Attaining whole-ecosystem warming using air and deep soil heating methods with an elevated CO₂ atmosphere. *Biogeosciences Discussions*, 1–48, 1–48. <https://doi.org/10.5194/bg-2016-449>
- Hayward, P. M., & Clymo, R. S. (1982). Profiles of water content and pore size in sphagnum and peat, and their relation to peat bog ecology. *Proceedings of the Royal Society of London. Series B: Biological Sciences*, 215(1200), 299–325. <https://doi.org/10.1098/rspb.1982.0044>
- Huang, Y., Jiang, J., Ma, S., Ricciuto, D., Hanson, P. J., & Luo, Y. (2017). Soil thermal dynamics, snow cover and frozen depth under five temperature treatments in an ombrotrophic bog: Constrained forecast with data assimilation. *Journal of Geophysical Research: Biogeosciences*, 122, 2046–2063. <https://doi.org/10.1002/2016JG003725>
- Humphreys, E. R., Andrew Black, T., Morgenstern, K., Li, Z., & Nesci, Z. (2005). Net ecosystem production of a Douglas-fir stand for 3 years following clearcut harvesting. *Global Change Biology*, 11(3), 450–464. <https://doi.org/10.1111/j.1365-2486.2005.00914.x>
- Iversen, C. M., Childs, J., Norby, R. J., Garrett, A., Martin, A., Spence, J., ... Latimer, J. (2017). *SPRUCE S1 Bog fine-root production and standing crop assessed with minirhizotrons in the southern and northern ends of the S1 Bog*. Oak Ridge, TN: Carbon Dioxide Information Analysis Center, Oak Ridge National Laboratory, U.S. Department of Energy. <https://doi.org/10.3334/CDIAC/spruce.019>
- Joabsson, A., Christensen, T. R., & Wallén, B. (1999). Vascular plant controls on methane emissions from northern peatforming wetlands. *Trees*, 14(10), 385–388. [https://doi.org/10.1016/S0169-5347\(99\)01649-3](https://doi.org/10.1016/S0169-5347(99)01649-3)
- Kang, H., Freeman, C., & Ashendon, T. W. (2001). Effects of elevated CO₂ on fen peat biogeochemistry. *Science of the Total Environment*, 279(1-3), 45–50. [https://doi.org/10.1016/S0048-9697\(01\)00724-0](https://doi.org/10.1016/S0048-9697(01)00724-0)
- Keenan, T. F., Carbone, M. S., Reichstein, M., & Richardson, A. D. (2011). The model-data fusion pitfall: Assuming certainty in an uncertain world. *Oecologia*, 167(3), 587–597. <https://doi.org/10.1007/s00442-011-2106-x>
- Keenan, T. F., Davidson, E. A., Munger, J. W., & Richardson, A. D. (2012). Rate my data: Quantifying the value of ecological data for the development of models of the terrestrial carbon cycle. *Ecological Applications*, 23(1), 273–286. <https://doi.org/10.1890/12-0747.1>
- Kettunen, A., Kaitala, V., Lehtinen, A., Lohila, A., Alm, J., Silvola, J., & Martikainen, P. J. (1999). Methane production and oxidation potentials in relation to water table fluctuations in two boreal mires. *Soil Biology and Biochemistry*, 31(12), 1741–1749. [https://doi.org/10.1016/S0038-0717\(99\)00093-0](https://doi.org/10.1016/S0038-0717(99)00093-0)
- Leifeld, J., Steffens, M., & Galego-Sala, A. (2012). Sensitivity of peatland carbon loss to organic matter quality. *Geophysical Research Letters*, 39, L14704. <https://doi.org/10.1029/2012GL051856>
- Le Mer, J., & Roger, P. (2001). Production, oxidation, and consumption of methane by soils: A review. *European Journal of Soil Biology*, 37(1), 25–50. [https://doi.org/10.1016/S1164-5563\(01\)01067-6](https://doi.org/10.1016/S1164-5563(01)01067-6)

- Lenhart, T., Eckhardt, K., Fohrer, N., & Frede, H.-G. (2002). Comparison of two different approaches of sensitivity analysis. *Physics and Chemistry of the Earth, Parts A, B and C*, 27(9-10), 645–654. [https://doi.org/10.1016/S1474-7065\(02\)00049-9](https://doi.org/10.1016/S1474-7065(02)00049-9)
- Luo, Y., Ahlström, A., Allison, S. D., Batjes, N. H., Brovkin, V., Carvalhais, N., ... Finzi, A. (2015). Towards more realistic projections of soil carbon dynamics by Earth system models. *Global Biogeochemical Cycles*, 30(1), 40–56. <https://doi.org/10.1002/2015GB005239>
- Luo, Y., & Reynolds, J. F. (1999). Validity of extrapolating field CO₂ experiments to predict carbon sequestration in natural ecosystems. *Ecology*, 80(5), 1568–1583. [https://doi.org/10.1890/0012-9658\(1999\)080%5B1568:VOEFCE%5D2.0.CO;2](https://doi.org/10.1890/0012-9658(1999)080%5B1568:VOEFCE%5D2.0.CO;2)
- Luo, Y., Wan, S., Hui, D., & Wallace, L. L. (2001). Acclimatization of soil respiration to warming in a tall grass prairie. *Nature*, 413(6856), 622–625. <https://doi.org/10.1038/35098065>
- Luo, Y., Weng, E., Wu, X., Gao, C., Zhou, X., & Zhang, L. (2009). Parameter identifiability, constraint, and equifinality in data assimilation with ecosystem models. *Ecological Applications*, 19(3), 571–574. <https://doi.org/10.1890/08-0561.1>
- Machacova, K., Bäck, J., Vanhatalo, A., Halmeenmäki, E., Kolari, P., Mammarella, I., ... Pihlatie, M. (2016). Pinus Sylvestris as a missing source of nitrous oxide and methane in boreal forest. *Scientific Reports*, 6(1). <https://doi.org/10.1038/srep23410>
- Megonigal, J. P., & Schlesinger, W. H. (1997). Enhanced CH₄ emission from a wetland soil exposed to elevated CO₂. *Biogeochemistry*, 37(1), 77–88. <https://doi.org/10.1023/A:1005738102545>
- Melton, J. R., Wania, R., Hodson, E. L., Poulter, B., Ringeval, B., Spahni, R., ... Eliseev, A. V. (2013). Present state of global wetland extent and wetland methane modelling: Conclusions from a model intercomparison project (WETCHIMP). *Biogeosciences*, 10(2), 753–788. <https://doi.org/10.5194/bg-10-753-2013>
- Meng, L., Hess, P. G. M., Mahowald, N. M., Yavitt, J. B., Riley, W. J., Subin, Z. M., ... Fuka, D. R. (2012). Sensitivity of wetland methane emissions to model assumptions: Application and model testing against site observations. *Biogeosciences*, 9(7), 2793–2819. <https://doi.org/10.5194/bg-9-2793-2012>
- Morrissey, L. A., & Livingston, G. P. (1992). Methane emissions from Alaska Arctic tundra: An assessment of local spatial variability. *Journal of Geophysical Research*, 97(D15), 16,661–16,670. <https://doi.org/10.1029/92JD00063>
- Neubauer, S. C., & Megonigal, J. P. (2015). Moving beyond global warming potentials to quantify the climatic role of ecosystems. *Ecosystems*, 18(6), 1000–1013. <https://doi.org/10.1007/s10021-015-9879-4>
- Oikawa, P. Y., Jenerette, G. D., Knox, S. H., Sturtevant, C., Verfaillie, J., Dronova, I., ... Baldocchi, D. D. (2016). Evaluation of a hierarchy of models reveals importance of substrate limitation for predicting carbon dioxide and methane exchange in restored wetlands. *Journal of Geophysical Research: Biogeosciences*, 122, 145–167. <https://doi.org/10.1002/2016JG003438>
- Pangala, S. R., Hornibrook, E. R., Gowing, D. J., & Gauci, V. (2015). The contribution of trees to ecosystem methane emissions in a temperate forested wetland. *Global Change Biology*, 21(7), 2642–2654. <https://doi.org/10.1111/gcb.12891>
- Parsekian, A. D., Slater, L., Ntarlagiannis, D., Nolan, J., Sebestyey, S. D., Kolka, R. K., & Hanson, P. J. (2012). Uncertainty in peat volume and soil carbon estimated using ground-penetrating radar and probing. *Soil Science Society of America Journal*, 76(5), 1911–1918. <https://doi.org/10.2136/sssaj2012.0040>
- Pitz, S., & Megonigal, J. P. (2017). Temperate forest methane sink diminished by tree emissions. *The New Phytologist*, 214(4), 1432–1439. <https://doi.org/10.1111/nph.14559>
- Richardson, A. D., Williams, M., Hollinger, D. Y., Moore, D. J. P., Dail, D. B., Davidson, E. A., ... Savage, K. (2010). Estimating parameters of a forest ecosystem C model with measurements of stocks and fluxes as joint constraints. *Oecologia*, 164(1), 25–40. <https://doi.org/10.1007/s00442-010-1628-y>
- Riley, W. J., Subin, Z. M., Lawrence, D. M., Swenson, S. C., Torn, M. S., Meng, L., ... Hess, P. (2011). Barriers to predicting changes in global terrestrial methane fluxes: Analyses using CLM4Me, a methane biogeochemistry model integrated in CESM. *Biogeosciences*, 8(7), 1925–1953. <https://doi.org/10.5194/bg-8-1925-2011>
- Roulier, S., & Jarvis, N. (2003). Analysis of inverse procedures for estimating parameters controlling macropore flow and solute transport in the dual-permeability model MACRO. *Vadose Zone Journal*, 2(3), 349–357. <https://doi.org/10.2136/vzj2003.3490>
- Saarnio, S., Järviö, S., Saarinen, T., Vasander, H., & Silvola, J. (2003). Minor changes in vegetation and carbon gas balance in a boreal mire under a raised CO₂ or NH₄NO₃ supply. *Ecosystems*, 6(1), 0046–0060. <https://doi.org/10.1007/s10021-002-0208-3>
- Saarnio, S., & Silvola, J. (1999). Effects of increased CO₂ and N on CH₄ efflux from a boreal mire: A growth chamber experiment. *Oecologia*, 119(3), 349–356. <https://doi.org/10.1007/s004420050795>
- Schipper, L. A., & Reddy, K. R. (1996). Determination of methane oxidation in the rhizosphere of *Sagittaria lancifolia* using methyl fluoride. *Soil Science Society of America Journal*, 60(2), 611–616. <https://doi.org/10.2136/sssaj1996.03615995006000020039x>
- Sebestyey, S. D., Dorrance, C., Olson, D. M., Verry, E. S., Kolka, R. K., Elling, A. E., & Kyllander, R. (2011). Long-term monitoring sites and trends at the Marcell Experimental Forest. In *Peatland Biogeochem. Watershed Hydrol. Marcell Exp. for* (pp. 15–72). Boca Raton, FL: CRC Press. <https://doi.org/10.1201/b10708-3>
- Sebestyey, S. D., & Griffiths, N. A. (2016). *SPRUCE Enclosure Corral and Sump System: Description, Operation, and Calibration*. Oak Ridge, TN: Climate Change Science Institute, Oak Ridge National Laboratory, U.S. Department of Energy. <https://doi.org/10.3334/CDIAC/spruce.030>
- Sebestyey, S. D., Verry, E. S., & Brooks, K. N. (2011). Hydrological responses to forest cover changes on uplands and peatlands. In *Peatland biogeochemistry and watershed hydrology at the Marcell Experimental Forest*, Peatland Biogeochemistry and Watershed Hydrology at the Marcell Experimental Forest (Chap. 13, pp. 401–432). New York: CRC Press. <https://doi.org/10.1201/b10708-14>
- Segers, R. (1998). Methane production and methane consumption: A review of processes underlying wetland methane fluxes. *Biogeochemistry*, 41(1), 23–51. Retrieved from <http://www.jstor.org/stable/1469307>
- Segers, R., & Kengen, S. W. M. (1998). Methane production as a function of anaerobic carbon mineralization: A process model. *Soil Biology and Biochemistry*, 30(8-9), 1107–1117. [https://doi.org/10.1016/S0038-0717\(97\)00198-3](https://doi.org/10.1016/S0038-0717(97)00198-3)
- Shannon, R. D., & White, J. R. (1994). A three-year study of controls on methane emissions from two Michigan peatlands. *Biogeochemistry*, 27(1), 35–60. <https://doi.org/10.1007/BF00002570>
- Shannon, R. D., White, J. R., Lawson, J. E., & Gilmour, B. S. (1996). Methane efflux from emergent vegetation in peatlands. *Journal of Ecology*, 84(2), 239–246. <https://doi.org/10.2307/2261359>
- Shea, K., Turetsky, M. R., & Waddington, J. M. (2010). *Quantifying diffusion, ebullition, and plant-mediated transport of CH₄ in Alaskan peatlands undergoing permafrost thaw*. Washington, DC: American Geophysical Union.
- Shi, X., Thornton, P. E., Ricciuto, D. M., Hanson, P. J., Mao, J., Sebestyey, S. D., ... Bisht, G. (2015). Representing northern peatland microtopography and hydrology within the Community Land Model. *Biogeosciences*, 12(21), 6463–6477. <https://doi.org/10.5194/bg-12-6463-2015>
- Shi, Z., Yang, Y., Zhou, X., Weng, E., Finzi, A. C., & Luo, Y. (2015). Inverse analysis of coupled carbon-nitrogen cycles against multiple datasets at ambient and elevated CO₂. *Journal of Plant Ecology*, 9(3), 285–295. <https://doi.org/10.1093/jpe/rtv059>
- Shurpali, N. J., & Verma, S. B. (1998). Micrometeorological measurements of methane flux in a Minnesota peatland during two growing seasons. *Biogeochemistry*, 40(1), 1–15. <https://doi.org/10.1023/A:1005875307146>

- Smith, M. J., Purves, D. W., Vanderwel, M. C., Lyutsarev, V., & Emmott, S. (2013). The climate dependence of the terrestrial carbon cycle, including parameter and structural uncertainties. *Biogeosciences*, *10*(1), 583–606. <https://doi.org/10.5194/bg-10-583-2013>
- Spahni, R., Wania, R., Neef, L., van Weele, M., Pison, I., Bousquet, P., ... van Velthoven, P. (2011). Constraining global methane emissions and uptake by ecosystems. *Biogeosciences*, *8*(6), 1643–1665. <https://doi.org/10.5194/bg-8-1643-2011>
- Terazawa, K., Ishizuka, S., Sakata, T., Yamada, K., & Takahashi, M. (2007). Methane emissions from stems of *Fraxinus Mandshurica* Var. *Japonica* trees in a floodplain forest. *Soil Biology and Biochemistry*, *39*(10), 2689–2692. <https://doi.org/10.1016/j.soilbio.2007.05.013>
- Tfaily, M. M., Cooper, W. T., Kostka, J. E., Chanton, P. R., Schadt, C. W., Hanson, P. J., ... Chanton, J. P. (2014). Organic matter transformation in the peat column at Marcell Experimental Forest: Humification and vertical stratification. *Journal of Geophysical Research: Biogeosciences*, *119*, 661–675. <https://doi.org/10.1002/2013JG002492>
- Tokida, T., Miyazaki, T., Mizoguchi, M., Nagata, O., Takakai, F., Kagemoto, A., & Hatano, R. (2007). Falling atmospheric pressure as a trigger for methane ebullition from peatland. *Global Biogeochemical Cycles*, *21*, GB2003. <https://doi.org/10.1029/2006GB002790>
- Turetsky, M. R., Treat, C. C., Waldrop, M. P., Waddington, J. M., Harden, J. W., & McGuire, A. D. (2008). Short-term response of methane fluxes and methanogen activity to water table and soil warming manipulations in an Alaskan peatland. *Journal of Geophysical Research*, *113*, G00A10. <https://doi.org/10.1029/2007JG000496>
- Updegraff, K., Bridgman, S. D., Pastor, J., Weishampel, P., & Harth, C. (2001). Response of CO₂ and CH₄ emissions from peatlands to warming and water table manipulation. *Ecological Applications*, *11*(2), 311–326. [https://doi.org/10.1890/1051-0761\(2001\)011%5B0311:ROCACE%5D2.0.CO;2](https://doi.org/10.1890/1051-0761(2001)011%5B0311:ROCACE%5D2.0.CO;2)
- Van Groenigen, K. J., Osenberg, C. W., & Hungate, B. A. (2011). Increased soil emissions of potent greenhouse gases under increased atmospheric CO₂. *Nature*, *475*(7355), 214–216. <https://doi.org/10.1038/nature10176>
- Verry, E. S. (1984). Microtopography and water table fluctuation in a sphagnum mire. In Proceedings of the 7th International Peat Congress, Dublin, Ireland. The Irish National Peat Committee / The International Peat Society (pp. 11–31).
- Verville, J. H., Hobbie, S. E., Chapin, F. S., & Hooper, D. U. (1998). Response of tundra CH₄ and CO₂ flux to manipulation of temperature and vegetation. *Biogeochemistry*, *41*(3), 215–235. <https://doi.org/10.1023/a:1005984701775>
- Waddington, J. M., Roulet, N. T., & Swanson, R. V. (1996). Water table control of CH₄ emission enhancement by vascular plants in boreal peatlands. *Journal of Geophysical Research*, *101*(D17), 22,775–22,785. <https://doi.org/10.1029/96JD02014>
- Walter, B. P., & Heimann, M. (2000). A process-based, climate-sensitive model to derive methane emissions from natural wetlands: Application to five wetland sites, sensitivity to model parameters, and climate. *Global Biogeochemical Cycles*, *14*(3), 745–765. <https://doi.org/10.1029/1999GB001204>
- Walter, B. P., Heimann, M., & Matthews, E. (2001). Modeling modern methane emissions from natural wetlands: 1. Model description and results. *Journal of Geophysical Research*, *106*(D24), 34,189–34,206. <https://doi.org/10.1029/2001JD900165>
- Wang, Y.-P., & Leuning, R. (1998). A two-leaf model for canopy conductance, photosynthesis and partitioning of available energy. I: Model description and comparison with a multi-layered model. *Agricultural and Forest Meteorology*, *91*(1–2), 89–111. [https://doi.org/10.1016/S0168-1923\(98\)00061-6](https://doi.org/10.1016/S0168-1923(98)00061-6)
- Wang, Y.-P., Leuning, R., Cleugh, H. A., & Coppin, P. A. (2001). Parameter estimation in surface exchange models using nonlinear inversion: How many parameters can we estimate and which measurements are most useful? *Global Change Biology*, *7*(5), 495–510. <https://doi.org/10.1046/j.1365-2486.2001.00434.x>
- Wang, Y.-P., Trudinger, C. M., & Enting, I. G. (2009). A review of applications of model–data fusion to studies of terrestrial carbon fluxes at different scales. *Agricultural and Forest Meteorology*, *149*(11), 1829–1842. <https://doi.org/10.1016/j.agrformet.2009.07.009>
- Wania, R., Ross, I., & Prentice, I. C. (2009). Integrating peatlands and permafrost into a dynamic global vegetation model: 1. Evaluation and sensitivity of physical land surface processes. *Global Biogeochemical Cycles*, *23*, GB3014. <https://doi.org/10.1029/2008GB003412>
- Wania, R., Ross, I., & Prentice, I. C. (2010). Implementation and evaluation of a new methane model within a dynamic global vegetation model: LPJ-WHyMe v1. 3.1. *Geoscientific Model Development*, *3*(2), 565–584. <https://doi.org/10.5194/gmd-3-565-2010>
- Weng, E., & Luo, Y. (2008). Soil hydrological properties regulate grassland ecosystem responses to multifactor global change: A modeling analysis. *Journal of Geophysical Research*, *113*, G03003. <https://doi.org/10.1029/2007JG000539>
- Whalen, S. C. (2005). Biogeochemistry of methane exchange between natural wetlands and the atmosphere. *Environmental Engineering Science*, *22*(1), 73–94. <https://doi.org/10.1089/ees.2005.22.73>
- Whalen, S. C., & Reeburgh, W. S. (1992). Interannual variations in tundra methane emission: A 4-year time series at fixed sites. *Global Biogeochemical Cycles*, *6*(2), 139–159. <https://doi.org/10.1029/92GB00430>
- Whiting, G. J., & Chanton, J. P. (1992). Plant-dependent CH₄ emission in a subarctic Canadian fen. *Global Biogeochemical Cycles*, *6*(3), 225–231. <https://doi.org/10.1029/92GB00710>
- Wilson, R. M., Hopple, A. M., Tfaily, M. M., Sebestyen, S. D., Schadt, C. W., Pfeifer-Meister, L., ... Hanson, P. J. (2016). Stability of peatland carbon to rising temperatures. *Nature Communications*, *7*, 13,723. <https://doi.org/10.1038/ncomms13723>
- Wythers, K. R., Reich, P. B., Tjoelker, M. G., & Bolstad, P. B. (2005). Foliar respiration acclimation to temperature and temperature variable Q₁₀ alter ecosystem carbon balance. *Global Change Biology*, *11*(3), 435–449. <https://doi.org/10.1111/j.1365-2486.2005.00922.x>
- Xu, T., White, L., Hui, D., & Luo, Y. (2006). Probabilistic inversion of a terrestrial ecosystem model: Analysis of uncertainty in parameter estimation and model prediction. *Global Biogeochemical Cycles*, *20*, GB2007. <https://doi.org/10.1029/2005GB002468>
- Yvon-Durocher, G., Allen, A. P., Bastviken, D., Conrad, R., Gudas, C., St-Pierre, A., ... del Giorgio, P. A. (2014). Methane fluxes show consistent temperature dependence across microbial to ecosystem scales. *Nature*, *507*(7493), 488–491. <https://doi.org/10.1038/nature13164>
- Zhang, Y., Li, C., Trettin, C. C., Li, H., & Sun, G. (2002). An integrated model of soil, hydrology, and vegetation for carbon dynamics in wetland ecosystems. *Global Biogeochemical Cycles*, *16*(4), 9–17. <https://doi.org/10.1029/2001GB001838>
- Zhu, Q., Liu, J., Peng, C., Chen, H., Fang, X., Jiang, H., ... Zhou, X. (2014). Modelling methane emissions from natural wetlands by development and application of the TRIPLEX-GHG model. *Geoscientific Model Development*, *7*(3), 981–999. <https://doi.org/10.5194/gmd-7-981-2014>
- Zhu, X., Zhuang, Q., Chen, M., Sirin, A., Melillo, J., Kicklighter, D., ... Song, L. (2011). Rising methane emissions in response to climate change in Northern Eurasia during the 21st century. *Environmental Research Letters*, *6*(4), 045211. <https://doi.org/10.1088/1748-9326/6/4/045211>
- Zhuang, Q., Melillo, J. M., Kicklighter, D. W., Prinn, R. G., McGuire, A. D., Steudler, P. A., ... Hu, S. (2004). Methane fluxes between terrestrial ecosystems and the atmosphere at northern high latitudes during the past century: A retrospective analysis with a process-based biogeochemistry model. *Global Biogeochemical Cycles*, *18*, GB3010. <https://doi.org/10.1029/2004GB002239>